


 Cite this: *Lab Chip*, 2026, 26, 1053

## Lab-on-a-chip for biomarker detection: advances, practical applications, and future perspectives

 Tianfeng Xu,<sup>†ab</sup> Hao Bai,<sup>ID†ab</sup> Jie Hu,<sup>†\*a</sup> Limei Zhang,<sup>a</sup> Weihua Zhuang,<sup>ID<sup>a</sup></sup>  
 Chang Zou,<sup>a</sup> Yongchao Yao,<sup>ID\*<sup>a</sup></sup> Wenchuang (Walter) Hu<sup>ID\*<sup>a</sup></sup> and Jin Huang<sup>\*b</sup>

Lab-on-a-chip (LoC) technology has emerged as a transformative platform for biomarker detection, integrating multiple analytical processes within a single microfluidic device. Advances in microfabrication and fluid dynamics have enabled the development of miniaturized, automated assays characterized by high sensitivity, rapid analysis, and portability. These advances facilitate diverse applications, including nucleic acid and protein analysis, as well as multiplexed biomolecular detection. LoC systems are particularly impactful for early cancer screening, infectious disease diagnostics, and real-time health monitoring. Integration with multi-omics approaches further enhances their capacity to elucidate complex disease mechanisms, thereby advancing precision medicine. Continued innovation in materials science, device architecture, and system integration promises to enhance the diagnostic performance, cost-effectiveness, and reliability of LoC systems across clinical settings. This review summarizes recent progress in LoC-based biomarker detection, highlighting innovations in fabrication, assay integration, and practical applications. It also discusses prevailing challenges and future research directions, offering insights into how LoC technology is poised to shape the next generation of precision diagnostics.

 Received 21st October 2025,  
 Accepted 16th December 2025

DOI: 10.1039/d5lc00986c

[rsc.li/loc](https://rsc.li/loc)

<sup>a</sup> Department of Laboratory Medicine, Precision Medicine Translational Research Center (PMTRC), West China Hospital, Sichuan University, Chengdu 610041, Sichuan, China. E-mail: hatuu@wchscu.edu.cn, huwenchuang@wchscu.cn  
<sup>b</sup> Department of Urology, Lab of Health Data Science, Innovation Institute for Integration of Medicine and Engineering, West China Hospital, Sichuan University, China. E-mail: michael\_huangjin@163.com

† These authors contributed equally to this work.

### 1. Introduction

As biomarkers become increasingly integral to precision medicine, the demand for rapid, sensitive, and point-of-care detection platforms has propelled lab-on-a-chip (LoC) systems into the spotlight.<sup>1,2</sup> They help in early disease detection, accurate diagnosis, treatment monitoring, and


**Yongchao Yao**

Yongchao Yao completed his PhD in Chemistry in 2019 under the supervision of Prof. Shiyong Zhang at Sichuan University. In 2020, he joined the laboratory of Prof. Zhiyong Qian for postdoctoral research at the same University. Dr Yao has published over 50 papers on international journals, including *Nat. Synth.*, *Nat. Commun.*, *Chemistry*, *Adv. Mater.*, *Angew. Chem., Int. Ed.*, *Chem. Sci.*, *Adv. Sci.*, *Chem. Mater.*, *Small*, *J. Mater. Chem. A*

*B*, *Chem. Commun.*, *Acta Biomater.*, *J. Energy Chem.*, *Anal. Chem.*, *Trends Anal. Chem.* and so on. Now his research activity primarily focuses on the rational design of functional nanostructures toward applications for medical devices, micro/nano biosensors, biochips, electrochemical high-throughput drug synthesis, etc.


**Wenchuang (Walter) Hu**

Wenchuang (Walter) Hu received a BSc degree in Electronics from the School of Electronics Engineering and Computer Science, Peking University, in 1999. He then obtained his PhD degree from the University of Notre Dame in 2002. During 2004–2005, he carried out postdoctoral research at the University of Michigan. Subsequently, in 2005 he joined the University of Texas at Dallas as an Assistant Professor and was

promoted to Professor in 2017. In 2021, he joined West China Hospital of Sichuan University as a full Professor. He published over 180 journal and conference papers. His research interests mainly focus on micro/nano biosensors, biosensors, biochips, nanomaterials, molecular diagnostic technologies, point-of-care testing, etc.

prognosis assessment.<sup>3,4</sup> Rapid, multiplexed LoC profiling also offers an enabling platform for large-scale longitudinal cohorts that demand repeated, minimally invasive sampling.<sup>5</sup> In contrast to conventional biomarker detection methods, including polymerase chain reaction (PCR), enzyme-linked immunosorbent assay (ELISA), and flow cytometry,<sup>6,7</sup> LoC technology stands out for its miniaturization, high integration, low sample requirement, and rapid automation.<sup>8</sup> These attributes enable LoC to facilitate portable, high-throughput, and multiplexed detection, thereby overcoming operational complexity.<sup>9,10</sup> Given these advantages, LoC technology is particularly well-suited to meet the demands of precision medicine and point-of-care testing.

LoC can manipulate extremely small fluid volumes ( $10^{-9}$  to  $10^{-18}$  liters), integrating multiple functions of traditional laboratories onto a small chip.<sup>11–13</sup> The core technologies of the LoC system include micro- and nano-fabrication, microfluidic manipulation, and biosensing. Micro- and nano-fabrication technology is used to fabricate various micro-nano structures on chips, such as microfluidic channels, microelectrodes, microsensors, *etc.*<sup>18</sup> Microfluidics enables precise liquid manipulation for sample transport, mixing, separation, and reaction control, which is necessary for blood separation, cell capture, and multi-step biochemical reaction integration.<sup>14</sup> Biosensing technology integrates biomarker recognition with signal converters to achieve *in situ* detection, fluorescent labeling detection, synchronous multiple detection, *etc.*<sup>15–17</sup> Compared to traditional laboratory techniques, LoC technology enables automated parallel processing of biological samples, allowing for the limitations of traditional approaches, which are often characterized by their bulkiness, time-consuming processes, and analysis of large datasets, and significant time savings.<sup>19,20</sup> Moreover, LoC reduces the dependence on laboratory sites, large equipment, and professional inspectors. This makes it

possible for patients to quickly complete self-screening of infectious diseases, tumor diseases, and dynamic self-inspection of chronic diseases. It also realizes the integrated closed-loop health management of hospital diagnosis and treatment and home monitoring, thereby effectively improving medical efficiency.<sup>21,22</sup>

In this review, we provide a comprehensive summary of the application of LoC technology in biomarker detection over the past few years, covering areas such as protein detection, nucleic acid detection, protein–nucleic acid multiplex detection, extracellular vesicle analysis, and more. Additionally, it also summarizes the latest developments in microfluidic manipulation, biosensing, micro- and nano-fabrication related to LoC technology, emphasizing their beneficial role in promoting the development of LoC technology for biomarker detection (Fig. 1). By achieving fast and accurate biomolecular analysis, LoC paves the way for advances in precision medicine, personalized treatment, and early diagnosis of diseases.

## 2. Technological development of LoC for biomarker detection

In recent years, LoC has undergone significant upgrades and optimizations based on various related technological advances. This section provides a summary of the latest developments in microfluidic manipulation, biosensing, and micro- and nano-fabrication related to LoC technology, highlighting their crucial role in advancing LoC systems for biomarker detection.

### 2.1 Micro- and nano-fabrication

The significant progress in the field of LoC is primarily attributed to innovations in micro- and nano-fabrication



Jin Huang

Jin Huang is the Executive Vice President of West China Hospital, Sichuan University, and Director of the Center for Medical-Engineering Innovation and Translation. He is a Leading Talent in Technological Innovation under Sichuan Province's "Tianfu Qingcheng Program" and serves as Vice Chair of the Medical Engineering Committee of the Chinese Medical Association and Vice President of the Chinese Society

of Medical Instrumentation. His research focuses on health cohort-based standards and digital diagnostics and therapeutics, with over 100 publications, and leadership of multiple national research projects.

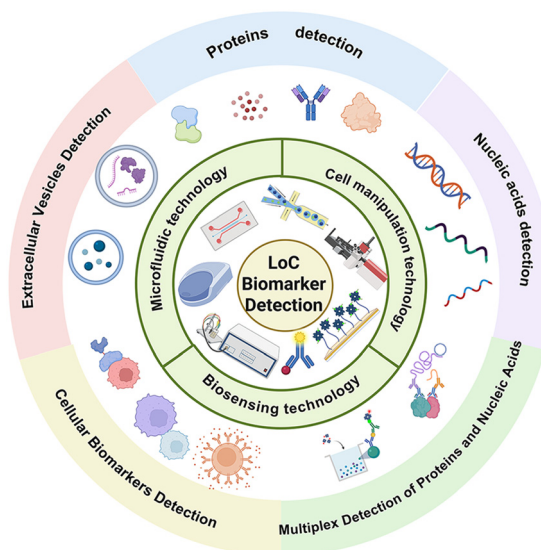


Fig. 1 Overview of multiple scenarios for biomarker detection in LoC (the figure is created in <https://BioRender.com>).

technology. These advancements have significantly improved the fabrication precision, cost-efficiency, and ease of production of microfluidic devices, as well as the effectiveness of surface modification techniques, thereby enhancing the overall performance and versatility of LoC platforms. Among the various fabrication methods, 3D printing, injection molding, and photolithography have emerged as pivotal technologies, each offering unique advantages and applications in LoC development.<sup>42</sup>

The application of 3D printing (Table 1) in LoC development confers substantial benefits, including cost-effectiveness, rapid prototyping, and exceptional design flexibility that enables customized and complex geometries. Such features make 3D printing especially advantageous during the research and development phase.<sup>45</sup> However, the relatively slow production rate and scalability limitations hinder its use in high-volume manufacturing, thereby restricting its broader industrial adoption.<sup>46,47</sup> For instance, Sharafeldin *et al.* developed a compact 3D-printed microfluidic chip that efficiently identifies and measures dengue NS1 protein using just 0.6 microliters of diluted human serum samples (at a 1:100 ratio) within a 30-minute timeframe.<sup>48</sup> Sinawang *et al.* have developed a 3D-printed microfluidic immunosensor array, which underwent several design refinements to optimize structural parameters and detection performance (Fig. 2A). In particular, they established a three-step post-processing protocol consisting of support removal, ultrasonic cleaning in isopropanol, and thermal curing at 60 °C. This procedure effectively eliminated uncured resin residues and reduced background fluorescence, thereby ensuring consistent printing resolution as well as stable surface functionalization for reliable assay performance. This device is capable of detecting five protein biomarkers associated with aggressive forms of cancer with exceptional sensitivity.<sup>49</sup>

Injection molding (Table 1) is an efficient mass production method suitable for manufacturing LoC devices with precise dimensions (Fig. 2B).<sup>50,51</sup> Researchers have introduced a technique for producing multi-tiered all-polymer microfluidic chips. This approach involves silicon dry etching, electroplating, and injection molding, resulting in channel depths from 100 nm to 100 μm. The structural

and material features of these devices directly support a range of biological applications. High-fidelity replication of high-aspect-ratio structures enables hydrodynamic confinement for both single-cell immobilization and parallel capture of large populations, meeting the needs of cell-based assays. The use of an optical-grade cyclic olefin copolymer with low autofluorescence provides a transparent background for real-time fluorescence microscopy, facilitating DNA elongation experiments in nanochannels. In addition, the integration of conductive polymer electrodes with robust bonding ensures leak-free perfusion under high pressures, which is essential for stable electrochemical monitoring of neurotransmitter release. The fabricated chips have been effectively utilized in cell capture, electrochemical analysis, and DNA extension applications.<sup>52</sup>

Photolithography (Table 1) is a traditional method for manufacturing microfluidic devices, transferring fine patterns on silicon wafers or other materials through a photochemical process. With the improvement of accuracy, photolithography has been able to achieve smaller feature sizes, which is crucial for improving the integration and performance of LoC devices.<sup>53,54</sup> For example, Qavi *et al.* utilized a maskless photolithography technique to create microfluidic devices for urine-derived EV extraction. The surface micropatterns, featured with a herringbone design, were particularly efficient at slowing down fluid flow, while the randomly oriented nanowires generated substantial near-wall vorticity. This combination likely enhances particle mixing near the walls, potentially boosting EV extraction effectiveness (Fig. 2C).<sup>55</sup>

## 2.2 Microfluidic manipulation

The foundation function of LoC technology is microfluidic manipulation, which enables precise manipulation of fluids at the micrometer scale. This level of precision is indispensable for biological assays, as clinically relevant biomarkers vary widely from nanometer-scale molecules to micrometer-scale cells, necessitating highly adaptable microfluidic strategies. Microfluidic technology simplifies the demanding equipment requirements of traditional biological detection laboratories and greatly enhances inspection

**Table 1** Explanation of key technologies in sections 2.1 and 2.3

Technology	Key characteristics
3D printing	It enables rapid prototyping and highly customizable designs, making it ideal for research and development, though its production speed limits large-scale manufacturing
Injection molding	It is an efficient, high-precision method for mass production, capable of creating complex, multi-functional devices suitable for diverse biological applications
Photolithography	It offers exceptional precision for creating miniaturized patterns, which is crucial for advancing device integration and performance, with emerging maskless techniques enhancing flexibility
Optical sensors ( <i>e.g.</i> , fluorescence, colorimetry)	They convert biological events into light-based signals, offering high sensitivity for multiplexed detection or low-cost, visual readouts for point-of-care testing
Electrochemical sensors	They translate binding events into electrical signals, valued for their low cost, low power consumption, and ease of integration, with advancing capabilities for multiplexed biomarker detection
Dual-mode sensors	They combine complementary sensing principles ( <i>e.g.</i> , optical and electrochemical) to provide cross-validated, more reliable results for complex samples, despite increased system complexity



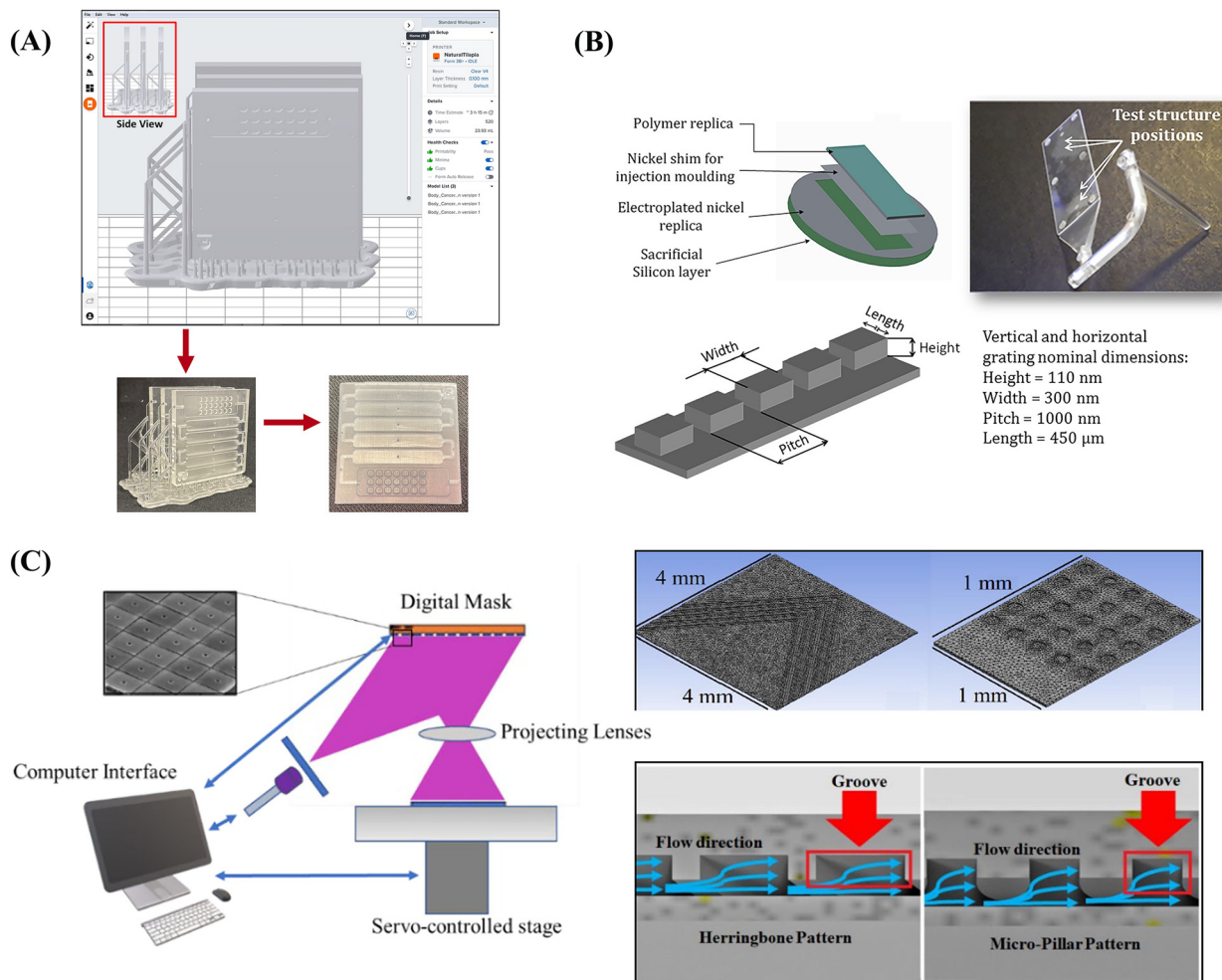


**Fig. 2** Representative innovative micro- and nano-manufacturing technologies for LoC devices. (A) Application of 3D printing technology in the design and manufacturing of microfluidic chips, reproduced from ref. 49 with permission from [MDPI], [P. D. Sinawang, *et al.*, *Sens. Actuators, B*, 2018, 259, 354–363, <https://doi.org/10.1016/j.snb.2017.12.043>], copyright 2018. (B) Injection molding is used for efficient mass production of LoC devices with precise dimensions, reproduced from ref. 50 with permission from [Institute of Physics Publishing], [K. Hiniduma, *et al.*, *Micromachines*, 2023, 14, 2187, <https://doi.org/10.3390/mi14122187>], copyright 2023. (C) Photolithography has been able to improve the integration and performance of LoC devices. For example, the herringbone design of surface micropatterns could slow down fluid flow, and the randomly oriented nanowires generated substantial near-wall vorticity, reproduced from ref. 55 with permission from [Elsevier], [I. Qavi, *et al.*, *Manuf. Lett.*, 2023, 35, 174–183, <https://doi.org/10.1016/j.mfglet.2023.08.008>], copyright 2023.

efficiency.<sup>23,24</sup> Overall, the forms of LoC can be divided into several principal categories, including lab-on-a-cartridge-chip, lab-on-a-disc, and microfluidic paper-based analytical devices ( $\mu$ PADs) (Fig. 3). These forms of LoC devices play a pivotal role in liquid biopsy by autonomously performing the entire workflow of biomarker separation, enrichment, and subsequent analysis.

The fundamental principle of LoC technology is the precise actuation of fluids, involving controlled initiation and termination of flow through valve mechanisms tailored to the device format. For lab-on-a-cartridge-chip, pneumatic-driven strategies such as self-balancing pressure chambers and burst valves are commonly deployed to sequentially regulate reagent release and mixing. For instance, Balaji *et al.* utilized standard soft lithography techniques to create microchannels connected to an array of microcavities for antibody–antigen

reactions. By leveraging the multiple inlets and outlets of their cartridge-style LoC, they connected external syringe pumps to impose a constant  $5 \mu\text{L min}^{-1}$  pressure-driven laminar flow, allowing precise metering of plasma samples and reagents through  $100 \mu\text{m} \times 50 \mu\text{m}$  microchannels; this active flow control enabled rapid and reliable quantification of glial fibrillary centrifugal forces and geometry to automate fluid progression.<sup>25</sup> In addition to conventional pneumatic actuation, lab-on-a-cartridge-chip devices can exploit electrowetting-on-dielectric (EWOD) to orchestrate droplet motion. Bai *et al.* employed an EWOD-driven L-junction electrode network to reproducibly split a  $60 \mu\text{L}$  mother droplet into eight uniform sub-droplets of  $5.68 \pm 0.28 \mu\text{L}$ . On a hydrophobic-coated, double-layer PCB-indium tin oxide chip, the team achieved fully automated metering, transport, coalescence, and thermal cycling of nanolitre-scale droplets,

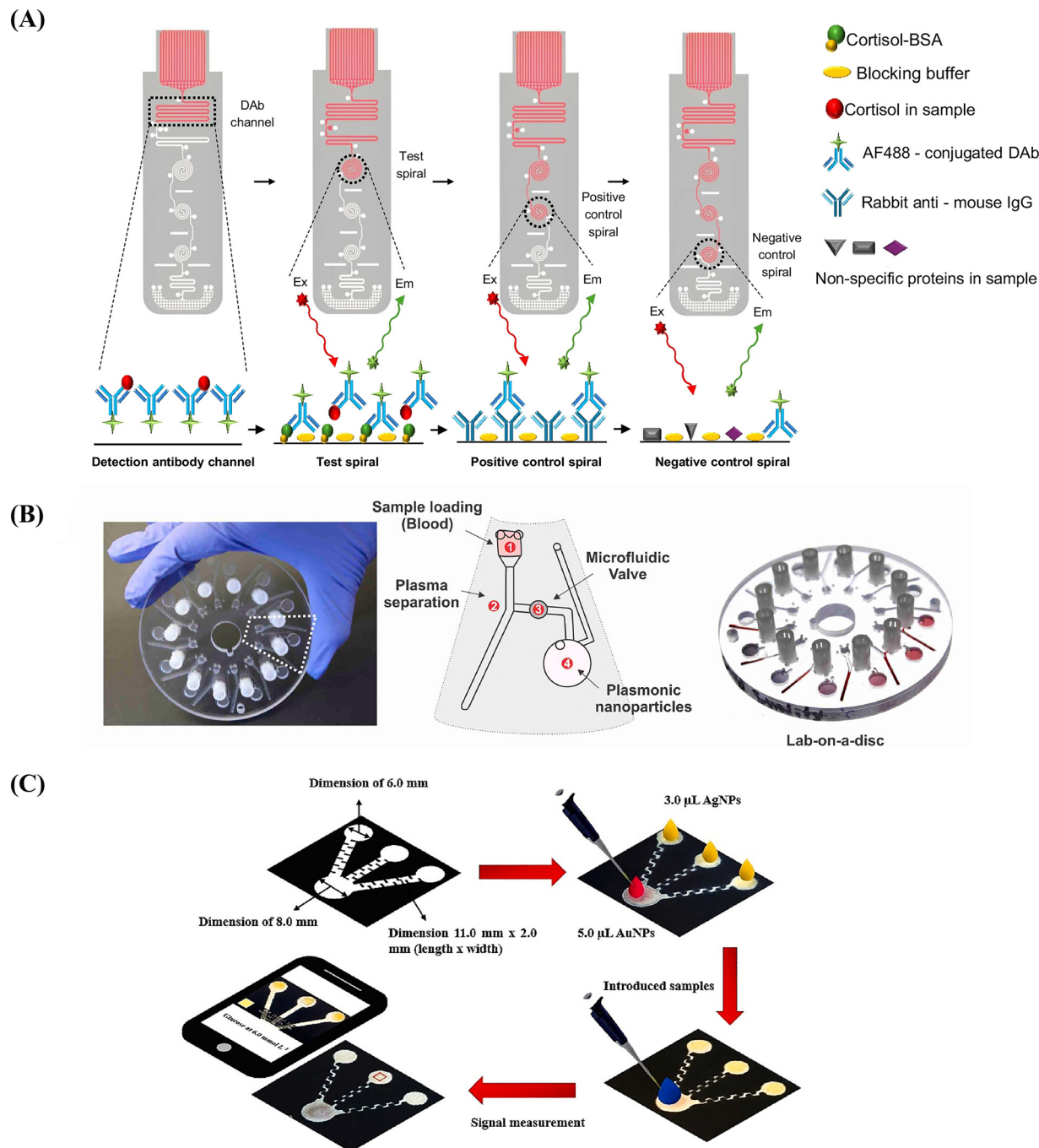


**Fig. 3** The working principles of three classic types of LoC systems for biomarker detection. (A) Lab-on-a-cartridge-chip: schematic of the fabricated LoC and steps for the fluorescence-based competitive cortisol immunoassay, adapted from ref. 24 with permission from [Elsevier], [V. T. Upaassana, *et al.*, *Biomed. Microdevices*, 2025, 27, 17, <https://doi.org/10.1007/s10544-025-00733-6>], copyright 2025. (B) Lab-on-a-disc: visual characterization of the microfluidic device for cysteamine detection, reproduced from ref. 26 with permission from [Elsevier], [H. Bai, *et al.*, *Lab Chip*, 2025, 25, 1552–1564, <https://doi.org/10.1039/d4lc00704b>], copyright 2025. (C)  $\mu$ PADs: paper microfluidic detection steps and methods, reproduced from ref. 27 with permission from [Elsevier], [M. Karmacharya, *et al.*, *Biosens. Bioelectron.*, 2021, 194, 113584, <https://doi.org/10.1016/j.bios.2021.113584>], copyright 2021.

completing the entire sample-to-PCR workflow without external pumps or valves.<sup>26</sup> In lab-on-a-disc platforms, fluid control is accomplished *via* passive valves. Utilizing centrifugal force, Karmacharya *et al.* developed a platform that directs blood radially outward to achieve plasma

separation, valve actuation, and reagent mixing autonomously, without external pumps or manual intervention.<sup>27</sup> Paper-based  $\mu$ PADs, by contrast, utilize capillary-driven flow, often enhanced with delay or stop valves implemented through hydrophobic patterning, wax

barriers, or EWOD, enabling controlled stepwise fluid delivery and multiplexed assays. Khachornsakkul *et al.* developed a paper-based  $\mu$ PAD that leverages the capillary action of paper fibers for pumpless fluid transport. Hydrophobic barriers, fabricated by wax printing and thermal reflow, define hydrophilic microchannels that guide the sample. Upon sample introduction, glucose is oxidized *via* an

enzyme-free cascade reaction to generate  $\text{H}_2\text{O}_2$ . The produced  $\text{H}_2\text{O}_2$  etches the gold nanoparticles, leading to an attenuation of the yellow color intensity, which serves as the analytical signal.<sup>28</sup> The  $\mu$ PADs address the demand for rapid, cost-effective, and portable biomarker detection and are extensively used for dynamic monitoring of various diseases.<sup>29</sup>

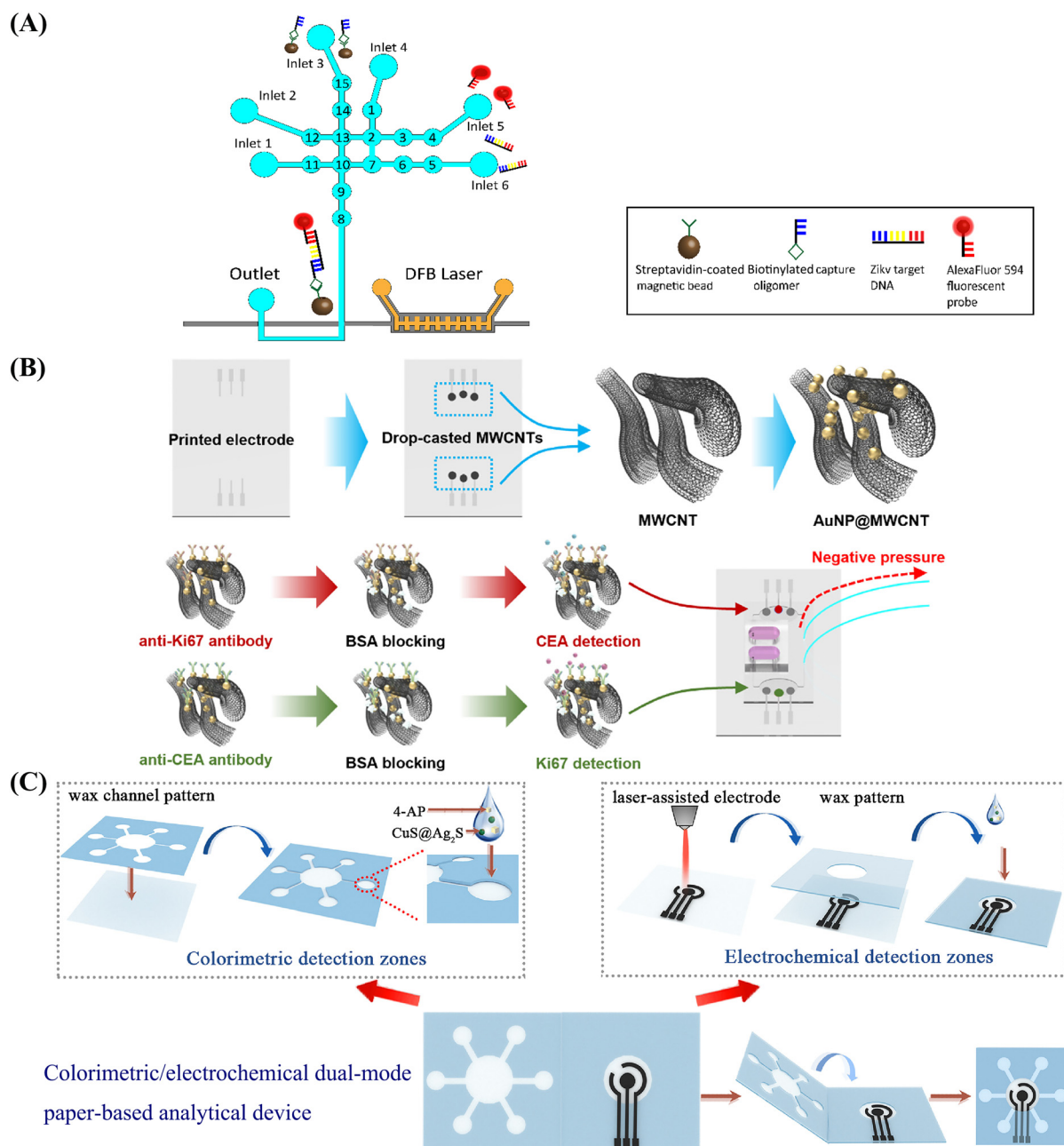


**Fig. 4** Biosensing technologies of LoC devices for biomarker detection: optical biosensors, electrochemical biosensors, and dual-mode biosensors. (A) Optical biosensors: a LoC integrated with an on-chip optical dye laser and optical detection technology was developed for specific Zika assay testing, reproduced from ref. 37 with permission from [MDPI], [L. A. García-Hernández, *et al.*, *Biosensors*, 2023, 13, 439, <https://doi.org/10.3390/bios13040439>], copyright 2023. (B) Electrochemical biosensors for multiplex detection: LoC with an anti-carcinoembryonic antigen (CEA) and anti-Ki67 antibody functionalized immunosensor, aiming to detect Ki67 and CEA, reproduced from ref. 41 with permission from [Elsevier], [B. Utzinger, *et al.*, *Lab Chip*, 2024, 24, 3802–3809, <https://doi.org/10.1039/d4lc00207e>], copyright 2024. (C) Dual-mode biosensors:  $\mu$ PADs for dual-mode DA analysis *via* colorimetric/electrochemical sensing, adapted from ref. 43 with permission from [Elsevier], [Z. Liu, *et al.*, *Biosens. Bioelectron.*, 2024, 263, 116558, <https://doi.org/10.1016/j.bios.2024.116558>], copyright 2024.



### 2.3 Biosensing modules in LoC systems

The biosensing module is a critical element of LoC systems, which provides the functional interface between target biomarkers and analytical readout.<sup>30–32</sup> The selection and integration of biosensors strongly determine the performance, cost, and clinical applicability of LoC devices.<sup>33,34</sup> Biosensing strategies can be broadly divided into optical, electrochemical, and dual-mode sensors.<sup>35,36</sup> Each category offers distinct advantages and trade-offs in terms of sensitivity, cost, stability, and suitability for POCT *versus* centralized laboratory diagnostics. This section highlights the working principles, integration considerations, and representative applications of these sensor types within LoC systems.

Optical biosensors (Table 1) utilize the principles of light-matter interaction to convert biological recognition events into quantifiable signals.<sup>37</sup> Fluorescence-based sensors enable high sensitivity and multiplexed detection, especially in nucleic acid sequencing. For instance, Sano *et al.* developed a LoC platform integrated with an on-chip optical dye laser and optical detection technology to capture and fluorescently labelled Zika virus nucleic acid. A magnetic bead assay was used in which beads carrying complementary DNA probes selectively captured Zika nucleic acids, followed by hybridization with fluorescent reporters to yield labeled constructs. The system produced highly specific fluorescence signals, with control experiments confirming the absence of false positives (Fig. 4A).<sup>38</sup> Colorimetric assays, though intrinsically limited by lower sensitivity and a narrower dynamic range than fluorescence, exploit nanozyme-driven chromogenic reactions to deliver low-cost, naked-eye readouts—attributes that render them uniquely suited for rapid POCT. Tai *et al.* developed a LoC device that employed a colorimetric biosensor that converted chloride- and glucose-induced color changes into quantifiable optical signals. By directly linking visible absorbance shifts to biomarker concentrations, it demonstrates the role of optical sensing in enabling rapid, low-cost, and portable diagnostics.<sup>39</sup> Electrochemical sensors (Table 1) are another common choice for on-chip biomarker detection. They are valued for being low-cost, power-efficient, and easily integrated into microfluidic systems.<sup>40</sup> For example, Utzinger *et al.* described a LoC, employing an electrochemical immunosensor based on screen-printed gold electrodes to detect serum C-X-C motif chemokine ligand 9 (CXCL9). Using a horseradish peroxidase (HRP)-catalyzed redox reaction that generated measurable oxidation currents, the device translated antigen-antibody binding into a quantitative electrical signal, achieving pg mL<sup>-1</sup> sensitivity.<sup>41</sup> Recent studies indicate that microfluidic-based electrochemical immunosensors can detect multiple biomarkers simultaneously with high sensitivity. Kim *et al.* developed a sensor platform using gold nanoparticles and a nanocomposite electrode. It enables simultaneous, quantitative detection of CEA and Ki-67, with a detection

limit of 0.97 ng mL<sup>-1</sup> (Fig. 4B).<sup>42</sup> This multiplexed detection could significantly influence future personalized medicine. In addition, LoC integrated with dual-mode biosensors (Table 1) is increasingly being applied in the field of biomarker detection.<sup>43</sup> Portable dual-mode  $\mu$ PADs integrating colorimetric and electrochemical detection were engineered for visual dopamine (DA) analysis. Featuring a folded design, they combine colorimetric and electrochemical detection layers fabricated *via* wax patterning and laser-induced graphene pyrolysis, facilitating vertical analyte transport. The  $\mu$ PADs demonstrate linear detection ranges of 2–50  $\mu$ M (colorimetric) and 0.5–70  $\mu$ M (electrochemical) for DA (Fig. 4C).<sup>44</sup> The superior capability of dual-mode platforms for confirmatory diagnostics and ultra-trace biomarker detection in complex samples justifies their use, despite higher associated complexity and cost.

## 3. Application of LoC in biomarker detection

LoC technology has emerged as a versatile platform for diverse biomarker detection. This chapter systematically summarizes LoC applications in protein detection, nucleic acid detection, multiplexed nucleic acid-protein detection, cellular biomarker detection, and EV detection.

### 3.1 Protein detection

Proteins play pivotal roles in diverse physiological and pathological processes within living organisms. They are integral to cellular functions, signal transduction, immune responses, and metabolic regulation.<sup>64–67</sup> Alterations in the expression levels and functional states of certain proteins often serve as key indicators of pathological mechanisms in disease states.<sup>67–69</sup> The detection of protein biomarkers has emerged as a crucial component in modern medical diagnostics and prognostics, enabling early disease detection, precise monitoring of disease trajectories, accurate assessment of treatment responses, and reliable prediction of patient outcomes.<sup>70,71</sup> Conventional protein assays such as ELISA, chemiluminescent immunoassay (CLIA), lateral flow immunoassays, and western blotting (WB) are limited by large sample requirements, multi-step protocols, and lengthy turnaround times.<sup>73,74</sup> LoC devices overcome these constraints through microfluidic integration of sample processing, reaction, and detection, enabling rapid and sensitive protein biomarker analysis (Table 2).<sup>72</sup>

**3.1.1 Immunoassay-based approaches.** Building upon conventional methods such as ELISA, LoC platforms have introduced significant improvements by miniaturizing reaction chambers, automating liquid handling, and reducing assay time. In 2013, Shim *et al.* developed a LoC platform that uniquely combines three microfabricated elements to deliver attomolar single-molecule immunoassays on a single PDMS chip.<sup>75</sup> As shown in Fig. 5A, LoC combined with bead-based ELISA was used for the detection of the

Table 2 The latest progress of LoC application in protein biomarker detection

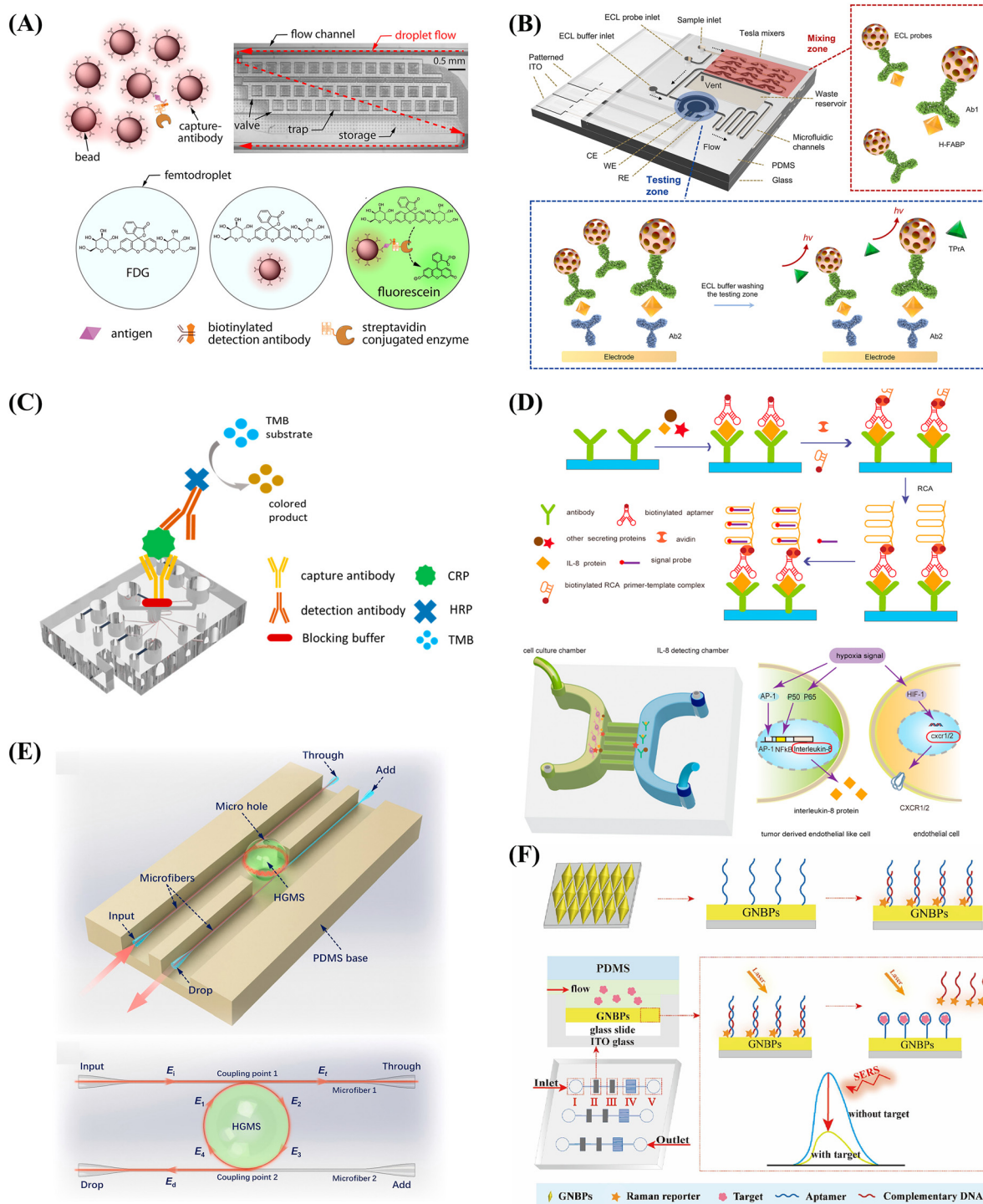
Year	Microfluidic platform	Fabrication technique	Sensing modality	Biomarker	Detection significance	Sample volume	Time required for detection	Linear range	LOD	Reference
2018	Lab-on-a-cartridge-chip	SU-8 photolithography	Optical biosensor (fluorescence)	Interleukin 8	Quickly diagnose inflammation and infection	10 $\mu\text{L}$	45 min (estimated value)	7.5–120 $\text{pg mL}^{-1}$	0.84 $\text{pM}$	82
2018	Lab-on-a-cartridge-chip	Photolithography	Optical biosensors (chemiluminescent/enzyme-amplified signal)	Interleukin-6, procalcitonin, and C-reactive protein	Quickly diagnose inflammation and infection	$\leq 5 \mu\text{L}$	20 min (estimated value)	From $\text{pg mL}^{-1}$ to $\mu\text{g mL}^{-1}$ , and 40 $\text{ng mL}^{-1}$	0.47 $\text{pg mL}^{-1}$ , 2.6 $\text{pg mL}^{-1}$ , and 40 $\text{ng mL}^{-1}$	83
2019	Lab-on-a-cartridge-chip	Injection molding	Optical biosensors (chemiluminescence)	Tumor necrosis factor $\alpha$	Early diagnosis of respiratory disease caused by respirable crystalline silica	20 $\mu\text{L}$	<30 min	Unknown	0.5 $\text{pg mL}^{-1}$	85
2020	Lab-on-a-cartridge-chip	3D printing	Optical biosensors (colorimetric)	VEGF, angiopoietin-2	Early diagnosis of initial cancer development and tumor metastasis	Unknown	2.5 h (estimated value)	Unknown	11 $\text{ng mL}^{-1}$ and 0.8 $\text{ng mL}^{-1}$	86
2020	Lab-on-a-cartridge-chip	Photolithography	Optical biosensor, bioluminescence resonance energy transfer (BRET)	Thrombin activity	Diagnosis and monitoring of coagulation-related diseases	23.6 $\mu\text{L}$	5 min	0.11 $\text{mU } \mu\text{L}^{-1}$ –1.69 $\text{mU } \mu\text{L}^{-1}$	38 $\mu\text{U } \mu\text{L}^{-1}$	87
2023	Lab-on-a-cartridge-chip	3D printing	Optical biosensor (colorimetric assays)	SARS-CoV-2 nucleocapsid protein	Rapid diagnosis of infectious diseases	210 $\mu\text{L}$	1.5 h	Unknown	For buffer: 54 $\text{pg mL}^{-1}$ , for diluted saliva: 91 $\text{pg mL}^{-1}$	76
2023	Lab-on-a-cartridge-chip	Photolithography, soft lithography, 3D printing	Optical biosensor	SARS-CoV-2 spike protein	Early distinction between COVID-19 and influenza	50 $\mu\text{L}$	15 min	SARS-CoV-2 spike protein: 100 $\text{fg mL}^{-1}$ –1 $\mu\text{g mL}^{-1}$	100 $\text{fg mL}^{-1}$	88
2023	Lab-on-a-cartridge-chip	Photolithography	Optical biosensor (SERS)	$\alpha$ -Synuclein, phosphorylated tau protein 181, osteopontin, and osteocalcin.	Early diagnosis of Parkinson's disease	10 $\mu\text{L}$	6 min	1 $\text{pg mL}^{-1}$ –1 $\mu\text{g mL}^{-1}$ (log-linear)	Less than the $\text{pg mL}^{-1}$ level	89
2023	Lab-on-a-cartridge-chip	Photolithography + soft lithography	Electrochemical sensors	H-FABP	Early diagnosis of acute myocardial infarction	300 $\mu\text{L}$	45 min	1–100 $\text{ng mL}^{-1}$	0.72 $\text{ng mL}^{-1}$	78
2023	Lab-on-a-cartridge-chip	Photolithography	SERS	PDGF-B, VEGF	Early assessment of tumor invasiveness	50 $\mu\text{L}$	20 min	Unknown	0.342 $\text{pg mL}^{-1}$ and 0.265 $\text{pg mL}^{-1}$	97
2024	Lab-on-a-cartridge-chip	Soft lithography	Optical biosensor (colorimetric assays)	Dust mite-specific immunoglobulin E	Quickly diagnose allergic diseases	30 $\mu\text{L}$	3.5 min	5.2 $\text{pg mL}^{-1}$ –10 $\text{ng mL}^{-1}$ (estimated value)	5.2–6.6 $\text{pg mL}^{-1}$	79
2024	Lab-on-a-cartridge-chip	Laser micromachining	Optical biosensor (colorimetric assays)	C-reactive protein	Quickly diagnose inflammation and infection	150 $\mu\text{L}$	<50 min	1–500 $\text{ng mL}^{-1}$ (high sensitivity) and 500–1500 $\text{ng mL}^{-1}$ (extended saturation region)	0.1 $\text{ng mL}^{-1}$	80



Table 2 (continued)

Year	Microfluidic platform	Fabrication technique	Sensing modality	Biomarker	Detection significance	Sample volume	Time required for detection	Linear range	LOD	Reference
2024	Lab-on-a-cartridge-chip	SU-8 photolithography + soft lithography	Optical biosensor (fiber-laser amplification)	Cardiac troponin I	Early diagnosis of acute myocardial infarction	<5 nL	15 min	Unknown	5 pg mL <sup>-1</sup>	96
2024	Lab-on-a-cartridge-chip	3D printing	Optical biosensors	SARS-CoV-2 S-protein, IgM, N-protein, IgG, and IgG	Rapid diagnosis of infectious diseases	Unknown	1 h	S-protein: 0.10–49.38 ng mL <sup>-1</sup> ; N-protein: 0.17–16.67 ng mL <sup>-1</sup> ; IgM: 0.69–5.56 ng mL <sup>-1</sup> ; IgG: 0.21–19.5 ng mL <sup>-1</sup>	0.01, 0.02, 0.69, and 0.61 ng mL <sup>-1</sup> , respectively.	90
2025	Lab-on-a-cartridge-chip	Photolithography	Optical biosensors	Matrix metalloproteinase-9 and interleukin-6	Early diagnosis and progression monitoring of precancerous lesions of gastric cancer	5 μL	20 min	10 <sup>-12</sup> –10 <sup>-6</sup> g mL <sup>-1</sup>	Levels down to the pg mL <sup>-1</sup>	91

fluorescent product of individual enzyme molecules with high sensitivity in only 10 minutes. A 10 × 5 μm flow-focusing nozzle accelerated local shear forces to generate monodisperse 5–50 fL water-in-oil droplets at 1.3 MHz – two orders of magnitude faster than previous devices. Monolithic pneumatic valves trapped and released over 2 × 10<sup>5</sup> droplets within 10 s, eliminating the need for mechanically etched femtoliter wells. Meanwhile, a 5 μm-deep trap array arranged droplets into a monolayer for epifluorescence readout of individual reactions. A decade later, a 3D-printed ELISA-on-a-chip system was developed that integrated a structurally encoded capillary aliquoting circuit (CAC) and a microfluidic chain reaction (MCR). This design automated, miniaturized, and parallelized the entire sandwich ELISA protocol without relying on external pumps, valves, or precise pipetting. Its modular structure includes aliquoting capabilities, simplifying chip loading and pipetting operations, and allowing for higher surfactant concentrations.<sup>76</sup> This system enables quantitative, high-sensitivity detection of the acute respiratory syndrome coronavirus type 2 (SARS-CoV-2) nucleocapsid protein in 4×-diluted saliva. Importantly, the impact of these advances extends beyond laboratory settings: the miniaturization and automation inherent to LoC platforms render them highly suitable for point-of-care protein diagnostics, where rapid, portable, and reliable detection is critical.<sup>77</sup> Examples include microfluidic electrochemiluminescence (ECL) assays for cardiac biomarkers and compact LoC devices achieving sub-10 pg mL<sup>-1</sup> sensitivity within minutes, underscoring their potential in real-time clinical decision-making.<sup>78</sup> As illustrated in Fig. 5B, the featured microfluidic ECL LoC device integrates a sandwich-type immunoassay using Ru(bpy)<sub>3</sub><sup>2+</sup>-loaded mesoporous silica nanoparticles as ECL reporters to detect heart-type fatty acid-binding protein (H-FABP). The findings from their microfluidic ECL device align well with the outcomes from clinical ELISA tests. Liu *et al.* integrated electronic, fluidic, mechanical, and detection modules to create a compact POCT platform with reciprocating fluid flow.<sup>79</sup> This system enables rapid antigen–antibody binding and fast immunodetection. Using dust mite-specific immunoglobulin E as an example, this device has a detection limit of 5.2–6.6 pg mL<sup>-1</sup> and a coefficient of variation below 3%. The entire detection process requires just 3.5 minutes. In addition to on-site detection of acute and severe diseases, the optimized LoC system, combined with the ELISA technology principle, is also used for monitoring chronic diseases, bringing great convenience to the daily medical care of patients. Chen SJ *et al.* presented a microfluidic immuno-biosensing platform for the rapid detection and quantification of C-reactive protein (CRP) in urine and serum samples.<sup>80</sup> This system comprises a microfluidic spectrum chip paired with a micro-spectrometer detection device. As illustrated in Fig. 5C, employing the ELISA technique, the microchip substrate is pre-coated with capture and detection antibodies, which facilitate immune complex formation with



**Fig. 5** Principles of protein detection based on LoC strategies. (A) LoC combined with bead-based ELISA for the detection of the fluorescent product of individual enzyme molecules, reproduced from ref. 75 with permission from [American Chemical Society], [J.-u. Shim, *et al.*, *ACS Nano*, 2013, 7, 5955–5964, <https://doi.org/10.1021/nn401661d>], copyright 2013. (B) The LoC system is integrated with microfluidics and electrochemiluminescence technology, aiming to detect heart-type fatty acid binding protein, reproduced from [Elsevier], [L. H. Zhu, *et al.*, *Talanta*, 2023, 262, 124626, <https://doi.org/10.1016/j.talanta.2023.124626>], copyright 2023. (C) A novel chemiluminescence immunoassay for protein detection using LoC, reproduced from ref. 80 with permission from [MDPI], [S. J. Chen, *et al.*, *Biosensors*, 2024, 14, 283, <https://doi.org/10.3390/bios14060283>], copyright 2024. (D) LoC significantly improved the sensitivity of protein detection by combining with RCA, reproduced from ref. 82 with permission from [Elsevier], [W. L. Zhang, *et al.*, *Biosens. Bioelectron.*, 2018, 102, 652–660, <https://doi.org/10.1016/j.bios.2017.12.017>], copyright 2018. (E) An optofluidic immuno-chip, incorporating fiber-laser enhancement technology to improve performance, reproduced from ref. 96 with permission from [Elsevier], [P. P. Niu, *et al.*, *Biosens. Bioelectron.*, 2024, 248, 115970, <https://doi.org/10.1016/j.bios.2023.115970>], copyright 2024. (F) LoC based on a SERS sensor, detecting PDGF-B and VEGF simultaneously, reproduced from ref. 97 with permission from [Elsevier], [M. Chen, *et al.*, *Microchem. J.*, 2023, 193, 109106, <https://doi.org/10.1016/j.microc.2023.109106>], copyright 2023.

the CRP antigen. This method enables the assessment of highly sensitive CRP levels within a 50-minute timeframe.

**3.1.2 Amplification-assisted detection.** Beyond accelerating traditional assays, LoC platforms harness molecular amplification strategies to tackle low-abundance protein detection. By confining techniques such as rolling circle amplification (RCA) and proximity ligation assay (PLA) within microfluidic architectures, these systems dramatically improve signal-to-noise ratios, enabling reliable detection of biomarkers at picogram concentrations. For instance, Gobet *et al.* established a high-throughput LoC platform that miniaturizes PLA to the nanoliter scale and enables 640 parallel reactions on a single multilayer PDMS device.<sup>81</sup> This approach significantly cuts reagent consumption and minimizes cross-contamination risks. It incorporates valve-based microfluidics, optimized surface chemistry, and precise thermal control to integrate DNA spotting, ligation, amplification, and fluorescence detection into a continuous automated workflow. Another key feature is the embedded RCA step, which substantially increases detection sensitivity. The platform allows reliable quantification of low-abundance protein biomarkers and facilitates high-throughput protein-interaction studies and validation. Furthermore, isothermal amplification and detection can be performed simultaneously within controlled microenvironments. Interleukin-8 (IL-8), a pro-inflammatory chemokine involved in neutrophil chemotaxis, is widely recognized as a biomarker of inflammatory diseases. Using a dual-function microfluidic biosensor with RCA, Zhang *et al.* developed a microfluidic chip.<sup>82</sup> As shown in Fig. 5D, immunoassays were performed *via* a sandwich structure comprising antibodies, IL-8, and aptamers, with signal amplification resulting from RCA and biotin–streptavidin linkage. In this assay, the linear detection range for IL-8 was 7.5–120 pg mL<sup>-1</sup>.

**3.1.3 Optical and nanostructured sensors.** In addition to miniaturized immunoassays and molecular amplification strategies, the integration of optical and nanostructured sensing technologies has further expanded the functionality of LoC platforms. Surface-enhanced Raman spectroscopy (SERS) enables sensitivity at the single-molecule level with minimal sample preparation and rapid analysis, making it a powerful biosensing approach.<sup>83,84</sup> Signal enhancement can be further optimized using high-precision piezoelectric lithographic devices that improve the performance of capture molecules on micropatterned or nanopatterned substrates.<sup>85,92–95</sup> Coupling microfluidics with approaches such as SERS, fiber-laser-based signal enhancement, and computational analysis enables highly sensitive, multiplexed, and real-time protein biomarker detection.<sup>92–95</sup> Niu *et al.* developed an optofluidic immunochip, leveraging fiber-laser-enhanced technology, aimed at swiftly detecting cardiac troponin I (within 15 minutes). This LoC platform combines whispering-gallery-mode microsphere resonators with fiber-laser amplification to achieve SERS-level sensitivity without using SERS (Fig. 5E). Its dual-stage optical mechanism, which merges high-Q resonance with external-cavity gain, narrows

spectral linewidth, improves signal-to-noise ratio by orders of magnitude, and lowers the detection limit to 5 pg mL<sup>-1</sup>.<sup>96</sup> Chen *et al.* developed a LoC with an SERS sensor, aiming at simultaneously detecting platelet-derived growth factor-B (PDGF-B) and vascular endothelial growth factor (VEGF). This LoC platform combines ordered gold nano-bipyramid (GNBP) arrays with competitive aptamer recognition for highly sensitive and multiplexed protein detection (Fig. 5F). Linearly self-assembled GNBP form uniform “hot-spot chains”, providing reproducible SERS enhancement. Dual-probe aptamer design allows VEGF and PDGF-B quantification *via* target-induced displacement of labelled complements, while a pump-free tri-channel, six-chamber microfluidic architecture ensures rapid, parallel sample handling. The platform delivers detection limits below 1 pg mL<sup>-1</sup> (VEGF: 0.342 pg mL<sup>-1</sup>; PDGF-B: 0.265 pg mL<sup>-1</sup>).<sup>97</sup>

Together, three key advances—microfluidic miniaturization for speed and portability, molecular amplification (*e.g.*, RCA/PLA) for sensitivity, and optical/nanostructured sensing for multiplexing and resolution—collectively push LoC performance beyond conventional lab standards. This integration enables rapid, sensitive, and multiplexed protein detection, opening avenues for POCT and clinical translation.

### 3.2 Nucleic acid detection

Nucleic acid detection is of paramount importance in the early diagnosis, prognosis assessment, and treatment monitoring of various diseases.<sup>98,99</sup> It provides crucial information about genetic mutations, pathogen identification, and gene expression profiles, enabling healthcare professionals to make informed decisions and develop personalized treatment plans.<sup>100,101</sup> Traditional nucleic acid detection methods, such as PCR and gel electrophoresis, have been widely used. However, the need for complex sample preparation, cumbersome instrumentation, and lengthy procedures hamper their feasibility for POCT in resource-constrained environments.<sup>102</sup> By integrating microfluidics, nanotechnology, and portable detection systems, LoC devices offer a miniaturized and automated platform for nucleic acid analysis.<sup>103,104</sup> These devices enable rapid sample processing, reduce reagent consumption, minimize human intervention, and enhance detection sensitivity and specificity.<sup>105</sup> In this section, the crucial technical principles, integration strategies, and practical applications of LoC devices in nucleic acid detection were summarized (Table 3).

As an automated molecular diagnostic device, the essence of LoC lies in executing nucleic acid extraction, amplification, and detection within a singular system.<sup>106</sup> The most challenging part is the nucleic acid extraction phase, which is crucial, as the quality of downstream experimental outcomes hinges on the purity of the template. Numerous automated or semiautomated nucleic acid extraction techniques based on microfluidics have been explored to facilitate effective POCT.

Table 3 The latest progress of LoC application in nucleic acid biomarker detection

Year	Microfluidic platform	Fabrication technique	Sensing modality	Biomarker	Detection significance	Sample volume	Time required for detection	Linear range/performance test coverage	LOD	Reference
2018	Lab-on-a-cartridge-chip	Photolithography	Electrochemical sensors (chronoamperometric)	Circulating tumor nucleic acid of prostate cancer	Early diagnosis and screening of tumors	100 $\mu$ L	30 min	50–1000 copies	50 copies	133
2019	Lab-on-a-cartridge-chip	CO <sub>2</sub> -laser ablation	Optomagnetic biosensor	Synthetic influenza target	Potential for rapid diagnosis of viral infections	100 $\mu$ L (estimated value)	75 min	Unknown	20 pM	115
2020	Lab-on-a-cartridge-chip	Photolithography + soft-lithography	Optical biosensor (fluorescent CRISPR-Cas13 readout)	Multiplexed nucleic acid	Rapid diagnosis of acute viral infection	20 $\mu$ L	$\leq$ 3 h (taking the Zika virus as an example)	Unknown	1 copy per $\mu$ L	125
2020	Lab-on-a-cartridge-chip	Standard CMOS process	Electrochemical sensor (ISFET proton detection)	Azole-resistant <i>Aspergillus fumigatus</i>	Optimize infection control strategies	10 $\mu$ L	$\leq$ 30 min	10 <sup>1</sup> –10 <sup>6</sup> copies per reaction ( $R^2 = 0.99$ )	10 copies per reaction	111
2021	Lab-on-a-cartridge-chip	Computer numerical control milling of poly(methyl methacrylate)	Optical/colorimetric biosensor	SARS-CoV-2 RNA	Rapid diagnosis of COVID-19 infection	1 mL	$\leq$ 60 min	470–4700 copies per mL	470 SARS-CoV-2 copies per mL	116
2021	Lab-on-a-cartridge-chip	Microfabrication	Optical biosensor (fluorescence imaging)	BK virus DNA	Early detection of infection and dynamic monitoring	10 $\mu$ L	2 h	3.0 $\times$ 10 <sup>-4</sup> –1.5 $\times$ 10 <sup>8</sup> copies per mL of BKV DNA	Unknown	135
2022	Lab-on-a-cartridge-chip	Photolithography	Optical biosensors (CRISPR-Cas13/Cas12)	21 viruses, including SARS-CoV-2, other coronaviruses.	Rapid diagnosis of acute viral infection	Unknown	3 h (taking the SARS-CoV-2 as an example)	100–10 <sup>6</sup> copies per $\mu$ L	100 copies per $\mu$ L	127
2022	Lab-on-a-cartridge-chip	3D printing	Electrochemical sensors	SARS-CoV-2 RNA	Monitoring of COVID-19 infection and immunity	450 $\mu$ L of the saliva mixture, 15 $\mu$ L of plasma-spiked saliva	2 h	0.8 RNA copies per $\mu$ L–2.3 $\times$ 10 <sup>5</sup> RNA copies per $\mu$ L	0.8 RNA copies per $\mu$ L	145
2023	Lab-on-a-cartridge-chip	Photolithography + e-beam evaporation	Optical biosensors (colorimetric assays)	SARS-CoV-2 and its variants, H1N1 influenza A virus, and various bacteria	Quickly diagnose infection	Unknown	13 min (taking the SARS-CoV-2 as an example)	5 RNA copies per $\mu$ L–8 $\times$ 10 <sup>5</sup> RNA copies per $\mu$ L	5 RNA copies per $\mu$ L	140
2023	Paper-based $\mu$ PADs	Wax printing + origami	Optical biosensors (colorimetric lateral-flow assay)	<i>Salmonella enterica</i>	Rapid diagnosis of foodborne diseases	Unknown	20 min	260 CFU mL <sup>-1</sup> –2.6 $\times$ 10 <sup>5</sup> CFU mL <sup>-1</sup>	260 CFU mL <sup>-1</sup>	117
2023	Paper-based $\mu$ PADs	Wax printing + PDMS	Optical biosensors (colorimetric lateral-flow assay)	<i>Campylobacter jejuni</i>	Rapid diagnosis of foodborne diseases	20–50 $\mu$ L	30 min	46 CFU mL <sup>-1</sup> –4.6 $\times$ 10 <sup>6</sup> CFU mL <sup>-1</sup>	460 CFU mL <sup>-1</sup>	118

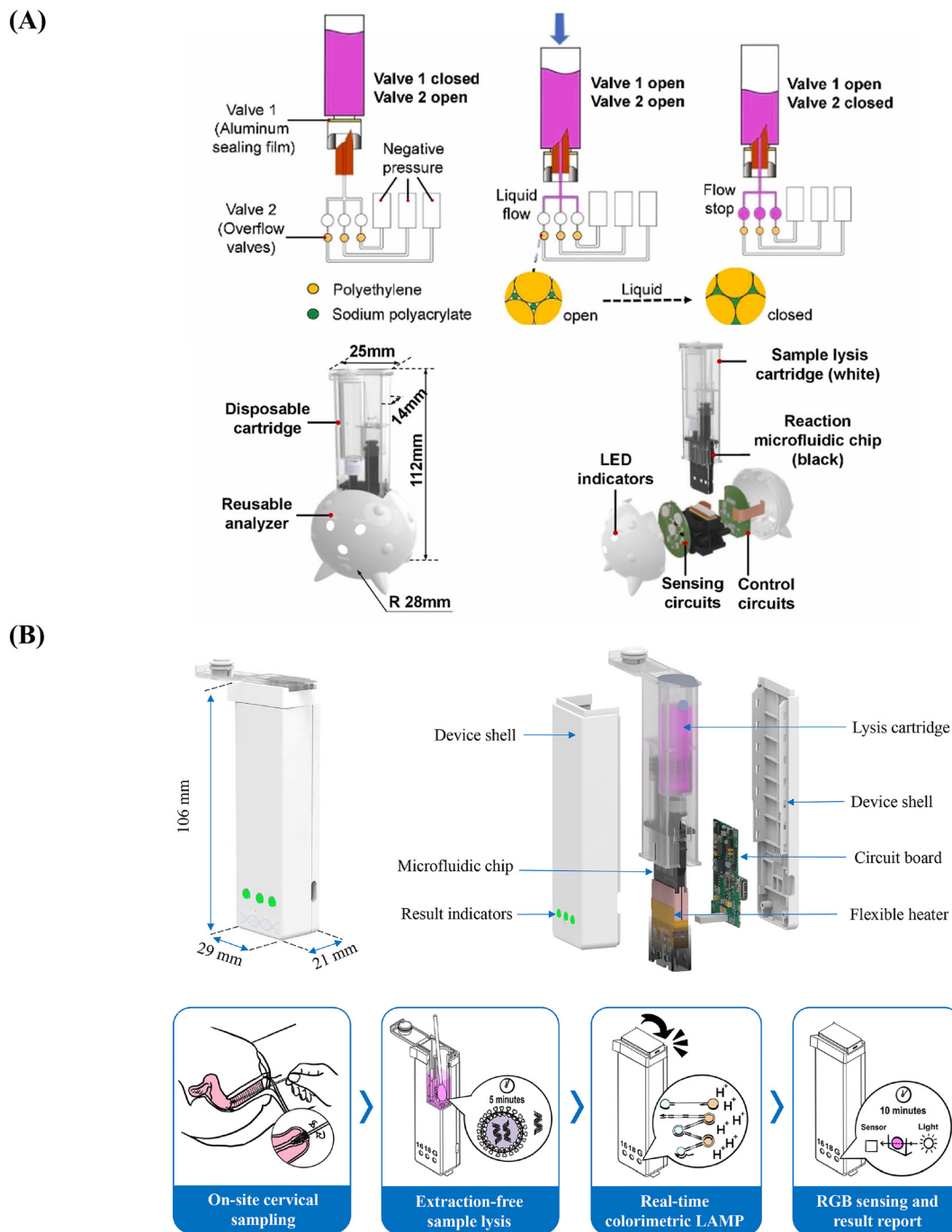


Table 3 (continued)

Year	Microfluidic platform	Fabrication technique	Sensing modality	Biomarker	Detection significance	Sample volume	Time required for detection	Linear range/performance test coverage	LOD	Reference
2024	Lab-on-a-cartridge-chip	Photolithography + soft-lithography	Optical biosensor (fluorescence)	EGFR gene (as validation)	Potential for rapid nucleic acid detection	25 $\mu\text{L}$	5 min	$1-10^4$ copies per $\mu\text{L}$	1 copy per $\mu\text{L}$	119
2024	Lab-on-a-cartridge-chip	3D printing	Optical biosensor (fluorescence)	Toxin genes A and B (pathogenic <i>Clostridioides difficile</i> )	Rapid diagnosis of <i>Clostridioides difficile</i> infection	12.4 $\mu\text{L}$	15 min	$10^1-10^7$ DNA molecules per reaction	119 to 1411 DNA molecules	121
2024	Paper-based $\mu\text{PADs}$	Wax printing + PDMS soft lithography	Optical biosensors (colorimetric lateral-flow assay)	Murine norovirus 1	Rapid diagnosis of foodborne diseases	50 $\mu\text{L}$	35 min	$2 \times 10^2-2 \times 10^5$ PFU $\text{mL}^{-1}$	200 PFU $\text{mL}^{-1}$	120
2025	Paper-based $\mu\text{PADs}$	Wax printing + PDMS soft lithography	Optical biosensors (colorimetric lateral-flow assay)	The H5/H7/H10 avian influenza virus	Subtype-specific discrimination of avian influenza virus	50 $\mu\text{L}$	20 min	Unknown	2 copies per reaction	122
2025	Lab-on-a-disc	CNC machining	Optical biosensor (fluorescence)	Pepper mild mottle virus	Preventing the spread of infectious diseases	100 $\mu\text{L}$	$\leq 1.5$ h	$6.0 \times 10^4-2.1 \times 10^7$ copies per mL	Unknown	123

In solid-phase extraction, magnetic or silica beads serve as a highly efficient method, as their large surface area is conducive to nucleic acid binding. Centrifugal microfluidics presents a strong alternative, with reagents stored in pressure-activated pouches or dried onto microchips in advance. It utilizes the centrifugal force generated by disk rotation to replace the external magnetic racks or electromagnets required in conventional magnetic bead-based methods, thereby enabling automated, low-contamination, and resource-efficient nucleic acid extraction, which is well-suited for POCT.<sup>107</sup> Isothermal amplification techniques – such as loop-mediated isothermal amplification (LAMP), recombinase polymerase amplification (RPA), and RCA – enable rapid nucleic acid detection without relying on thermal cyclers.<sup>108–113</sup> For example, LAMP employs DNA polymerase and four to six primers to amplify target DNA through DNA synthesis, strand displacement, and annealing processes at approximately 60–65 °C within 30–60 minutes.<sup>114</sup> These methods are well-suited for portable diagnostic applications due to their simplicity and minimal instrumentation requirements. In parallel, LoC systems enhance nucleic acid testing through integrated, miniaturized, and automated fluidic handling, accommodating both isothermal and PCR amplification. The combination of isothermal amplification with LoC technology improves both portability and operational efficiency, facilitating effective nucleic acid testing in field settings.<sup>128</sup> Leveraging these field-deployable advantages, research teams across the globe have translated the technology into a diverse array of distinctive LoC platforms tailored for POCT. Our group integrated extraction-free sample lysis, LAMP, and real-time colorimetric detection into a sealed chip for SARS-CoV-2 testing, hitting 53 copies per mL LOD (Fig. 6A).<sup>129</sup> In subsequent studies by the same group, Bai *et al.* achieved autonomous HPV16/18 testing in 15 minutes without pipetting, centrifugation or biosafety equipment. The platform achieves single-copy sensitivity with 92% clinical sensitivity and 99% specificity, providing true sample-in-result-out capability at the most resource-limited point of care (Fig. 6B).<sup>130</sup> Costantini *et al.* developed a LoC device that conducted real-time reverse transcriptase PCR on RNA extracted from human viruses.<sup>137</sup> Compared to a standard thermal cycler, this system can detect RNA at identical concentrations, with the time required for PCR analysis being half that of conventional methods.

In addition to single nucleic acid biomarker detection, the detection of multiple pathogens has received increasing attention recently.<sup>139</sup> For instance, combining LAMP with supercritical angle fluorescence micro-optic structures allows for spatial division in a multiplex setup, enabling the identification of multiple pathogens such as *Campylobacter coli*, *Salmonella* spp., *Campylobacter* spp., *Campylobacter jejuni*, and avian influenza virus (AIV).<sup>138</sup> Ackerman *et al.* created a combinatorial array for multiplexed nucleic acid detection, integrating it with Cas13 detection to distinguish 169 human-associated viruses (Fig. 7A).<sup>125</sup> T. AbdElFatah *et al.* created a LoC system for nucleic acid detection,



**Fig. 6** Representative LoC applications driving POCT innovation. (A) Working principle and zone layout of the LoC platform for viral infection detection and surveillance, reproduced from ref. 129 with permission from [Elsevier], [J. Hu, *et al.*, *Sens. Actuators, B*, 2024, **411**, 135740, <https://doi.org/10.1016/j.snb.2024.135740>], copyright 2024. (B) Overview of the LoC for HPV16/18 POCT: 15-minute sample-to-result workflow, exploded view, and dimensions of the credit-card-sized device, reproduced from ref. 130 with permission from [Elsevier], [H. Bai, *et al.*, *Biosens. Bioelectron.*, 2024, **248**, 115968, <https://doi.org/10.1016/j.bios.2023.115968>], copyright 2024.

leveraging plasma nanostructured surfaces and microfluidic technology. This device supports single-step LAMP and RCA reactions, enabling a ninefold acceleration of DNA/RNA amplification. It facilitates automated multiplex detection, capable of identifying respiratory pathogens like SARS-CoV-2 and its variants, H1N1 influenza A virus, and various bacteria, delivering highly accurate results (95%) within just

13 minutes.<sup>140</sup> Ahmadi *et al.* developed a LoC utilizing real-time reverse transcription PCR for non-extraction sample preparation, capable of detecting multiple pathogens, including SARS-CoV-2, influenza A/B, and respiratory syncytial virus. It demonstrated high consistency with conventional methods ( $R^2 = 0.983$ ) and offered a cost-effective approach to efficiently identify respiratory infections

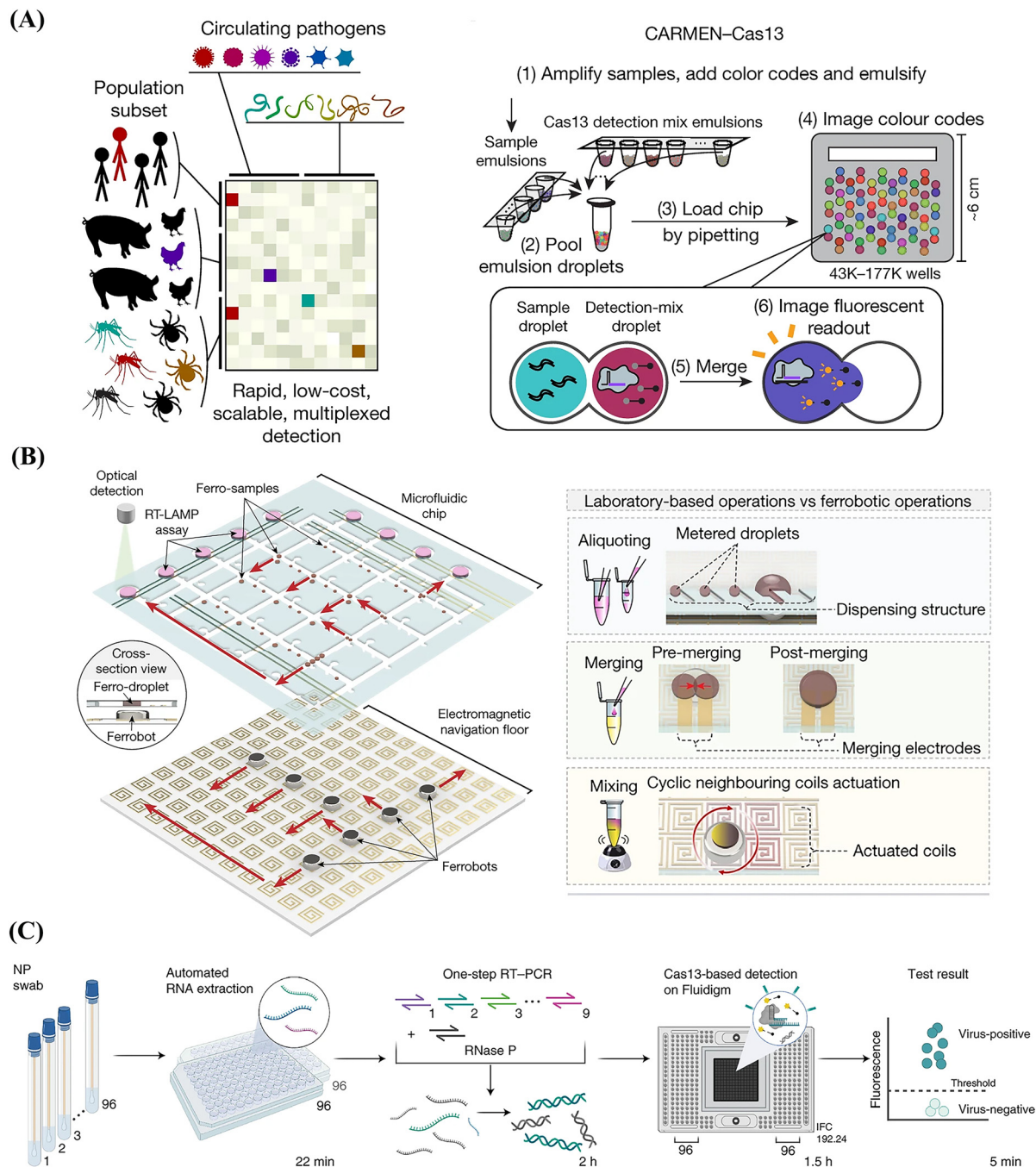


**Fig. 7** Classic automated workflow demonstration of LoC for nucleic acid biomarker detection. (A) A LoC platform integrated with Cas13 and arrayed reactions, referred to as CARMEN, has been developed for scalable and highly multiplexed pathogen detection, reproduced from ref. 125 with permission from [Springer Nature], [C. M. Ackerman, *et al.*, *Nature*, 2020, 582, 277–282, <https://doi.org/10.1038/s41586-020-2279-8>], copyright 2020. (B) A LoC integrates a microfluidic chip filled with oil and a printed circuit board with 2D coils. These coils can be individually controlled to manipulate ferrobots, enabling automated liquid handling, reproduced from ref. 126 with permission from [Springer Nature], [H. Lin, *et al.*, *Nature*, 2022, 611, 570–577, <https://doi.org/10.1038/s41586-022-05408-3>], copyright 2022. (C) Schematic of the Cas13-based LoC workflow for detecting 9 human respiratory viruses, reproduced from ref. 127 with permission from [Springer Nature], [N. L. Welch, *et al.*, *Nat. Med.*, 2022, 28, 1083–1094, <https://doi.org/10.1038/s41591-022-01734-1>], copyright 2022.

with similar clinical characteristics, thereby rapidly informing clinical decision-making.<sup>141</sup> While LoC platforms have demonstrated great potential in POCT,<sup>124</sup> recent advances have substantially broadened their capabilities, particularly in high-throughput screening and cost-effective

nucleic acid analysis. For instance, in another study, a group of millimeter-sized magnets was employed to accurately control magnetized sample droplets and reliably execute adaptable nucleic acid amplification processes, resulting in an approximately 1000-fold reduction in instrumentation



costs (Fig. 7B).<sup>126</sup> Welch *et al.* successfully implemented high-throughput detection of numerous viruses and their variants by integrating CRISPR-based diagnostics with microfluidics, with results closely matching those obtained through sequencing-based variant classification across 2088 patient samples (Fig. 7C).<sup>127</sup>

In addition, LoC platforms are particularly valuable for handling complex biological samples, such as cell-free DNA (cfDNA) and raw urine, by integrating crucial sample preparation steps alongside molecular detection. For instance, cfDNA – short DNA fragments released into bodily fluids through apoptosis or necrosis – serves as a critical biomarker for cancer screening and monitoring.<sup>131,132</sup> However, its low abundance and fragmentation necessitate highly sensitive and integrated detection systems. Koo *et al.* carried out liquid biopsy in a LoC, utilizing nanofluid control to accelerate solid-phase isothermal amplification and employing nanozyme-based electrochemical detection. This method can detect as low as 50 copies of circulating tumor nucleic acid of prostate cancer within 30 minutes, demonstrating the potential for rapid liquid biopsy.<sup>133</sup> Similarly, the detection of viruses like BK polyomavirus (BKV) in urine is technically challenging due to the presence of inhibitors and low target concentrations.<sup>134</sup> Xu *et al.* designed a LoC incorporating thermal control and fluorescence imaging modules, which quantifies BKV from raw urine without complex nucleic acid extraction or purification. This system could finish detection within 2 h, with a detection range of BKV DNA from  $3.0 \times 10^4$  to  $1.5 \times 10^8$  copies per mL.<sup>135</sup> Further expanding the scope, Chu *et al.* designed a LoC based on Fusion 5 paper discs, featuring a streamlined detection method for HCV RNA, which simplified the assay protocol while maintaining high clinical sensitivity and specificity. In a validation study with 60 clinical samples, the device demonstrated 100% performance on both metrics, with a detection limit of approximately 101 IU mL<sup>-1</sup>.<sup>136</sup>

### 3.3 Multiplex detection of proteins and nucleic acids

The simultaneous detection of proteins and nucleic acids holds substantial clinical significance. This integrated approach facilitates precise disease identification, reveals underlying pathological mechanisms, and pinpoints potential drug targets, thereby enabling tailored therapeutic interventions.<sup>142</sup> Unlike conventional methods that often require sequential processing and separate assays for nucleic acids and proteins, LoC devices enable rapid and parallel analysis of multiple analytes. This parallel processing capability significantly reduces the analysis time, expediting the diagnostic process. However, the actual research and development of the LoC platform poses considerable challenges. It must achieve high-sensitivity and high-specificity detection for diverse biomolecules, while also addressing critical issues such as signal interference and detection efficiency.<sup>143</sup> Currently, its application scope remains limited, primarily focused on the diagnosis and monitoring of infectious diseases. During the COVID-19

outbreak, the rapid and accurate detection of both SARS-CoV-2 RNA (from respiratory samples) and host antibodies (from serum) is critical for clinical diagnosis, helping confirm active infections and assess immune status in recovering patients.<sup>144</sup> For example, Najjar *et al.* designed a 3D-printed LoC device that achieves this goal. The saliva sample requires no specialized pre-treatment for antibody detection on this platform. It is simply mixed with a small volume of plasma at a 1:20 ratio and loaded directly. Then, a single saliva sample is split into two parallel microfluidic paths: one aliquot ( $\approx 15 \mu\text{L}$ ) flows over the antigen-coated electrodes for sandwich electrochemical ELISA serology, while a larger aliquot ( $\approx 280 \mu\text{L}$ ) is processed for RNA extraction, amplification, and CRISPR-based detection (Fig. 8A).<sup>145</sup> With the further development of integrated technology for sample preparation and detection, an acoustofluidic integrated molecular diagnostics LoC was engineered. This device enables fast and sensitive detection of viral immunoglobulins, including IgA, IgG, and IgM, alongside nucleic acids. Utilizing acoustic vortices and Gor'kov potential wells, it concurrently isolates viruses and antibodies from saliva samples. Notably, it has nearly a 100% recovery rate for viruses and antibodies, offers a detection limit of 15.6 pg mL<sup>-1</sup> for immunity markers, and enhances RNA detection by 32-fold (Fig. 8B).<sup>146</sup>

### 3.4 Small molecule biomarker detection

Small molecule biomarkers have become essential in the biomedical field, facilitating disease diagnosis, treatment monitoring, and elucidation of physiological and pathological mechanisms.<sup>56</sup> These biomarkers encompass a wide range of molecules, including endogenous metabolites, amino acids and their derivatives, hormones, toxins, and drug molecules.<sup>57</sup> Their metabolomics is particularly significant in precision medicine, guiding personalized drug treatments to enhance efficacy and minimize toxicity.<sup>58,59</sup> However, these biomarkers are often present in low abundance and require advanced, costly laboratory equipment for detection. The emergence of LoC technologies has streamlined detection, enabling on-site production and utilization.

Various LoC platforms have been applied in the field of small-molecule biomarker detection, demonstrating excellent performance. Phenylketonuria (PKU) is characterized by a metabolic abnormality of phenylalanine hydroxylase in the bloodstream, causing psychomotor retardation. Akyilmaz *et al.* have engineered a portable diagnostic LoC capable of precisely detecting phenylalanine in whole blood within 20 minutes. The sensitivity of the measurement was enhanced by 1.5-fold through electrode modification, which was achieved *via* electrochemical reduction of graphene oxide and its subsequent deposition onto the electrode surface.<sup>60</sup> Lee *et al.* developed a wearable LoC platform for on-body detection of the hormone biomarker, cortisol. This facilitates non-invasive, continuous cortisol monitoring, aiding in long-term assessment of chronic stress-related conditions and



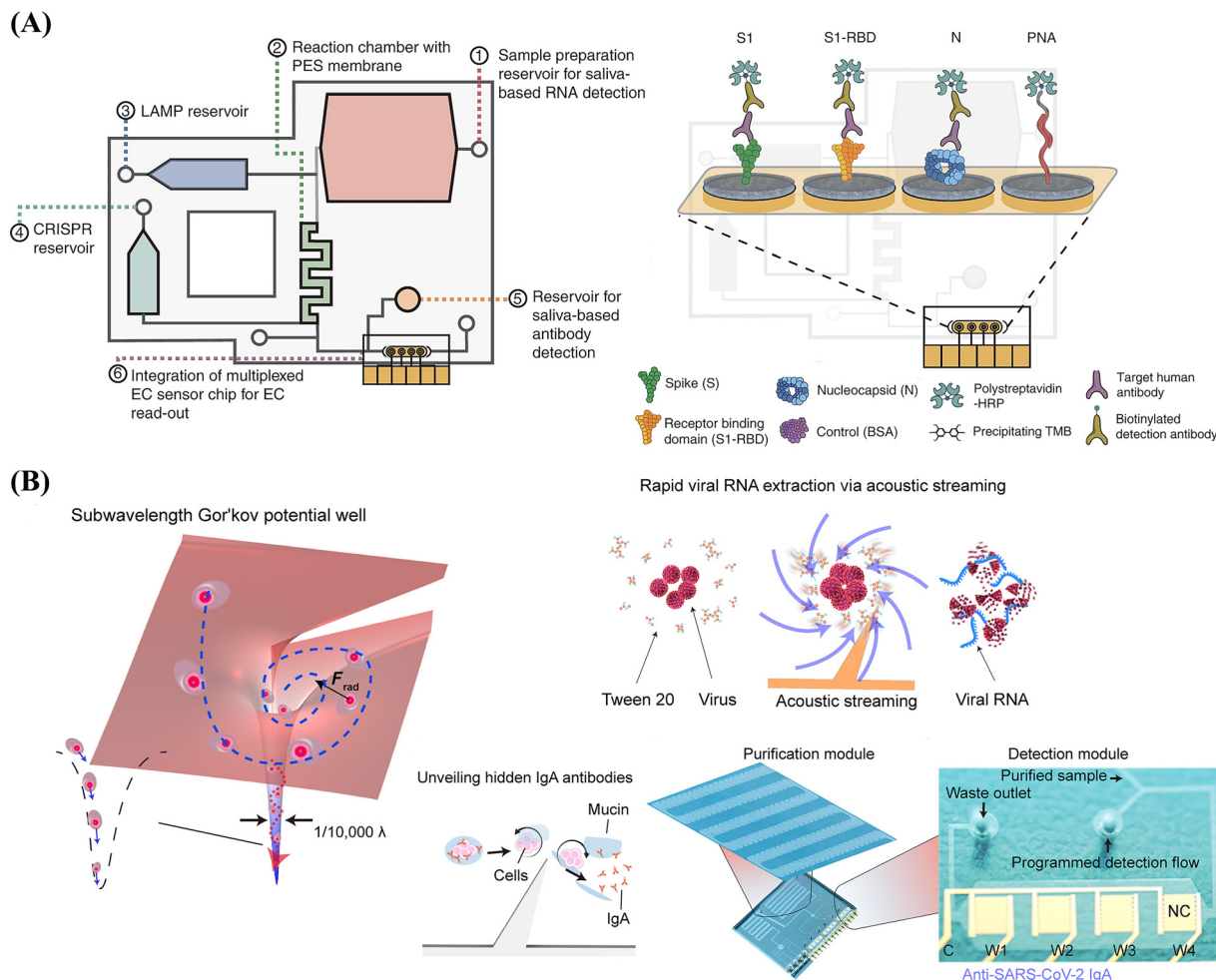


**Fig. 8** Multiplex detection of proteins and nucleic acids based on LoC. (A) A LoC for the simultaneous electrochemical detection of SARS-CoV-2 RNA and anti-SARS-CoV-2 antibodies, reproduced from ref. 145 with permission from [Springer Nature], [D. Najjar, *et al.*, *Nat. Biomed. Eng.*, 2022, 6, 968–978, <https://doi.org/10.1038/s41551-022-00919-w>], copyright 2022. (B) Acoustofluidic integrated molecular diagnostics LoC, enabling fast and sensitive detection of viral immunoglobulins alongside nucleic acids, reproduced from ref. 146 with permission from [American Association for the Advancement of Science], [J. Qian, *et al.*, *Sci. Adv.*, 2025, 11, eadt5464, <https://doi.org/10.1126/sciadv.adt5464>], copyright 2025.

guiding glucocorticoid therapy for patients.<sup>61</sup> Additionally, the portable detection of drug metabolites in LoC greatly promotes dynamic monitoring of therapeutic efficacy and toxicity prevention. For example, Narang *et al.* designed an electrochemical  $\mu$ PAD for diazepam detection, *via* synthesizing silica-coated gold nanorods (Si@GNRs). It demonstrated reliable detection of diazepam over a concentration range from 3.5 nM to 3.5 mM.<sup>62</sup> Korzhenko *et al.* developed a combination of a microfluidic electrochemical chip with an integrated mixer, enabling the detection of isomers of acetaminophen metabolites in a few minutes.<sup>63</sup> In this way, the toxicity risk of drugs can be more accurately evaluated, significantly more efficiently than conventional separation methods.

### 3.5 Cellular biomarker detection

Recent advances in cancer immunology and single-cell analysis demand technologies for monitoring dynamic

cellular biomarkers with ultrahigh sensitivity and spatiotemporal resolution. LoC systems address the limitations of conventional methods by integrating microfluidics, nanotechnology, and biosensing into miniaturized platforms. A crucial prerequisite for such analyses is the ability to efficiently isolate and manipulate rare cells, such as circulating tumor cells (CTCs), from complex biological samples.<sup>150–152</sup> To this end, LoC technologies have been developed for high-precision cell separation and enrichment. For example, Ma *et al.* designed an integrated microfluidic LoC platform that isolates epithelial ovarian cancer CTCs using antibody-conjugated magnetic nanoparticles, followed by quantification of nine malignancy-associated mRNAs *via* droplet digital PCR.<sup>153</sup> In another study, Ilayda

Namli *et al.* introduced a label-free LoC approach for CTC detection, where differential inlet pressures induce vapor bubble nucleation, and cavitation signatures serve as a biophysical marker for rapid CTC identification (Fig. 9B).<sup>154</sup>

These examples highlight the capacity of LoC systems to perform rare-cell separation as a foundation for subsequent molecular interrogation.

Building upon cell separation, LoC platforms further enable multiplexed biomarker detection and functional profiling at the single-cell level.<sup>147,148</sup> By integrating microfluidics with advanced biosensing modules, these systems allow precise surface protein profiling and real-time analysis of secretory biomarkers in picoliter volumes at single-molecule sensitivity. For instance, Gupta *et al.* developed a cost-effective droplet-based microfluidic system coupled with flow cytometry, which employs fluorescently labeled antibodies to sensitively detect cell surface biomarkers, such as the major histocompatibility complex (MHC) protein, at single-cell resolution (Fig. 9A).<sup>149</sup> Collectively, these innovations underscore the role of LoC technologies in bridging rare-cell separation with

downstream biomarker detection, thereby advancing the progress of precision medicine.

### 3.6 Extracellular vesicle detection

EVs are membrane-enclosed structures actively secreted by cells into the extracellular environment.<sup>155,156</sup> The biological molecules they carry, such as proteins, nucleic acids, and lipids, can be taken up by recipient cells.<sup>157,158</sup> This process modulates the physiological functions of these cells and influences cell-to-cell interactions.<sup>159–164</sup> Achieving final EV separation remains a significant challenge due to their small size and heterogeneity. The traditional EV separation methods are hindered by the presence of lipoproteins in plasma samples, which complicate downstream analysis and affect the accuracy of EV liquid biopsy.<sup>165,166</sup> To address this issue, Del Río *et al.* developed an integrated LoC device for

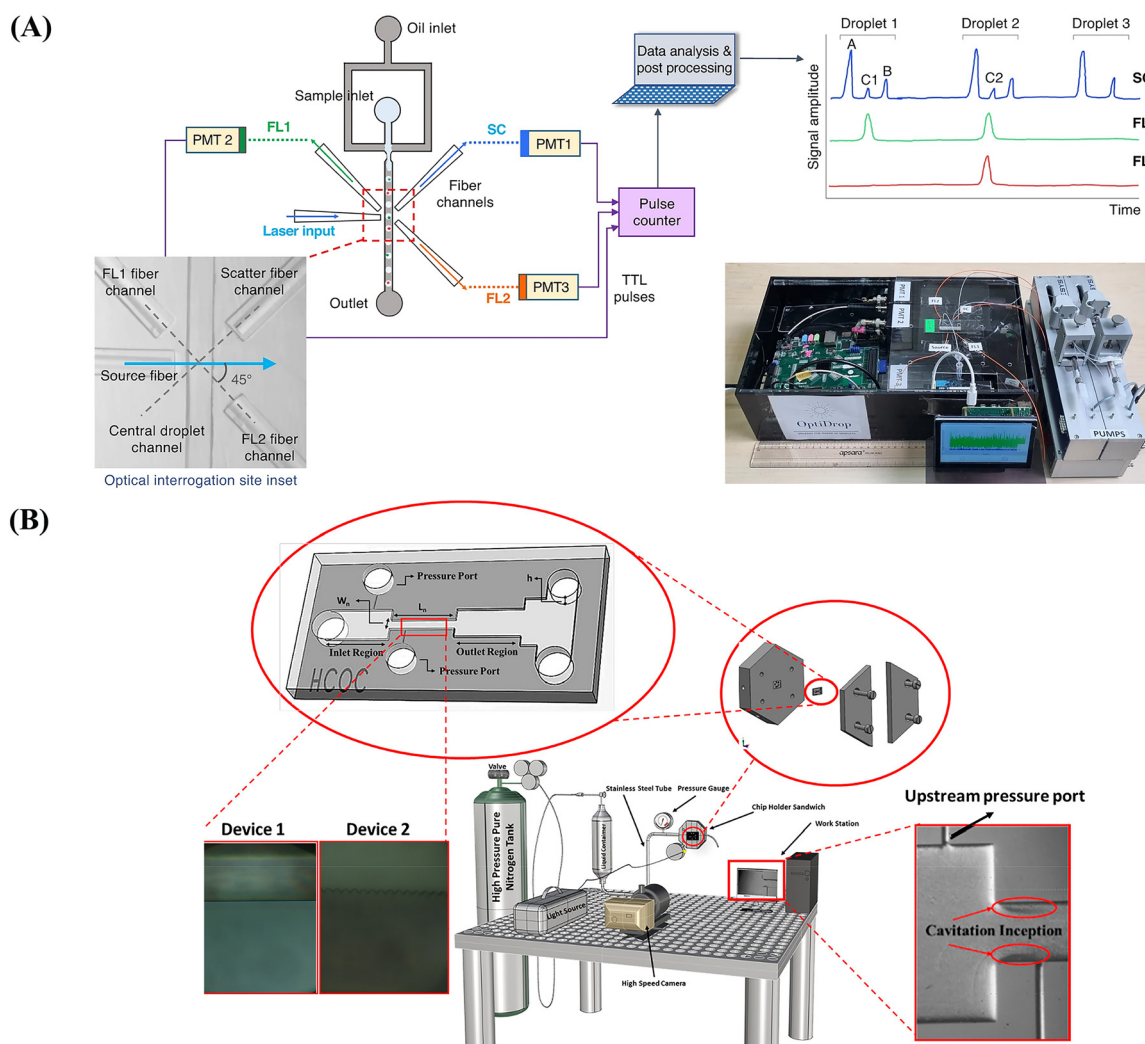


**Fig. 9** Cellular biomarkers detection based on LoC. (A) A novel cost-effective LoC combined with a droplet microfluidic platform and flow cytometry to recognize cell surface biomarkers, reproduced from ref. 149 with permission from [Springer Nature], [P. Gupta, *et al.*, *Microsyst. Nanoeng.*, 2024, 10, 35, <https://doi.org/10.1038/s41378-024-00665-w>], copyright 2024. (B) A LoC platform for CTC detection, utilizing differential inlet pressures triggering vapor bubble nucleation as fluids traverse the system, reproduced from ref. 154 with permission from [ACS Publications], [I. Namli, *et al.*, *ACS Appl. Mater. Interfaces*, 2022, 14, 40688–40697, <https://doi.org/10.1021/acsami.2c12356>], copyright 2022.

EV detection using DEP purification (Fig. 10A).<sup>167</sup> Similarly sized EVs and lipoprotein particles were isolated from blood plasma *via* centrifugal disc filtration. Subsequently, the

fractions were routed to a microfluidic chip containing slanted interdigitated electrodes. Different from the DEP principles, Ji *et al.* developed a LOC with monolayer-

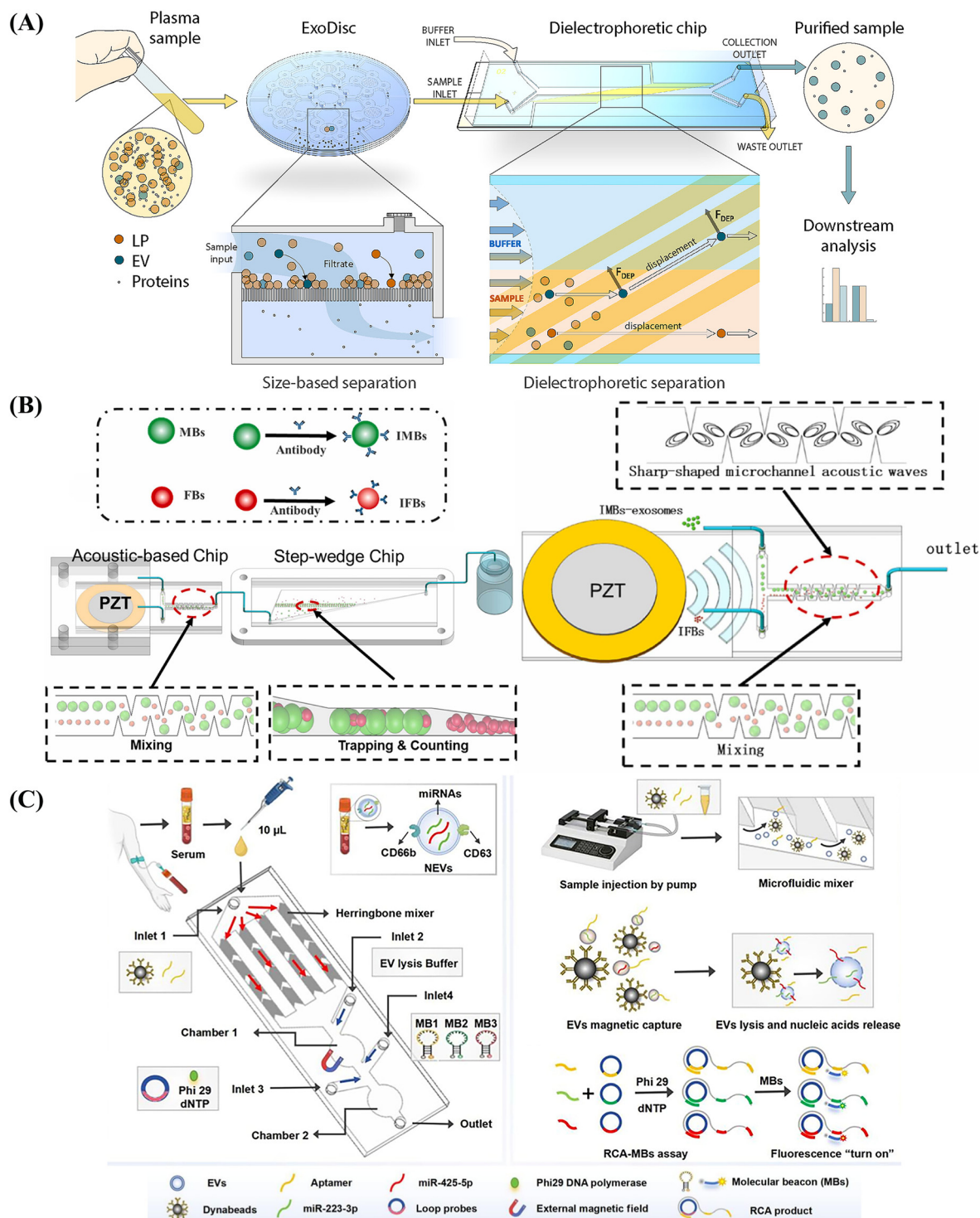


**Fig. 10** Extracellular vesicles detection based on LoC. (A) An integrated LoC *via* DEP purification technology for EV detection, reproduced from ref. 167 with permission from [American Chemical Society], [J. S. del Rio, *et al.*, *Langmuir*, 2024, 40, 25772–25784, <https://doi.org/10.1021/acs.langmuir.4c02098>], copyright 2024. (B) LOC with monolayer-fluorescence counting technology for ultrasensitive EV detection, reproduced from ref. 168 with permission from [Elsevier], [C. X. Ji, *et al.*, *Sens. Actuators, B*, 2025, 423, 136786, <https://doi.org/10.1016/j.snb.2024.136786>], copyright 2025. (C) A LoC-RCA platform for neutrophil-derived EV detection, adapted from ref. 172 with permission from [American Chemical Society], [D. Yu, *et al.*, *ACS Nano*, 2025, 19, 10078–10092, <https://doi.org/10.1021/acsnano.4c16894>], copyright 2025.



fluorescence counting technology for ultrasensitive EV detection. An integrated acoustic wave microchannel enhanced the mixing of the magnetic-EV complexes with antibody-conjugated fluorescent beads. The detection signal of the fluorescence-labelled immune sandwich complex can be read by counting, thus avoiding background interference and achieving a LOD of 850 particles per mL (Fig. 10B).<sup>168</sup> In another study, a magnetic nanoparticle-based LoC was presented for EV detection. This platform utilizes bubble-induced microagitation to enhance immunomagnetic bead-EV interactions, bypassing manual pipetting and external oscillatory incubation. During the verification process of model EVs, it performed 75.8% target capture yield and 62.7% recovery efficiency.<sup>169</sup>

Small EVs serve as valuable biomarkers for early-stage tumor detection and monitoring. Lan *et al.* introduced a DEP-based LoC platform incorporating optically transparent micro-beads to generate engineered electric field gradients. This platform can complete the quantification of EVs within 15 minutes, requiring only 20–50  $\mu\text{L}$  of samples, with a LOD of 161 particles per  $\mu\text{L}$ .<sup>170</sup> In another study, a 7-microchannel LoC integrated with SERS was developed to detect the phenotype changes of small EVs, leading to early diagnosis of ovarian carcinoma with high sensitivity and specificity. Antibody-functionalized SERS probes enabled multiplex biomarker recognition, encompassing universal EV markers and ovarian cancer-associated antigens (EpCAM, CD24, CA125, EGFR).<sup>171</sup> Yu *et al.* reported a LOC-RCA platform for

detecting neutrophil-derived EVs. Post-capture thermolysis released neutrophil-derived EV (NEV) aptamers and miRNAs, initiating on-chip RCA. CD66b<sup>+</sup> NEV could be separated from 10  $\mu\text{L}$  of serum, and the detected EV-derived miRNA could effectively distinguish gastric cancer, benign conditions, and healthy controls (Fig. 10C).<sup>172</sup>

Exosomes, a representative type of EVs, are common disease-related biomarkers in liquid biopsy.<sup>173–176</sup> Chinnappan *et al.* developed a dynamic LoC system employing a microfluidic magnetic field applied perpendicular to the flow direction, aiming to detect exosomes for early diagnosis of colorectal cancer.<sup>176</sup> Anti-CD63 aptamer-functionalized magnetic nanobeads served as recognition elements. Continuous flow combined with magnetic forces generated repetitive capture-release cycles during operation, ultimately completing exosome detection with an LOD of 1457 particles per mL. EVs are also considered biomarkers for the management of cardiovascular disease. Cheng *et al.* created a LoC platform incorporating high-sensitivity field-effect transistors for early diagnosis of cardiovascular disease. This system executed integrated EV processing – extraction, lysis, miRNA isolation, and detection – within 5 hours.<sup>177</sup> Recently, a LoC bionano-device based on Raman spectroscopy and artificial intelligence (AI) algorithms was reported for EV detection. It delivers real-time multiplex profiling of EV biomarkers, achieving >96% sensitivity and specificity for rapid diagnosis of cardiovascular disease.<sup>178</sup>

**Table 4** Comparison of biomarker detection: LoC-based methods *versus* conventional methods

Feature	LoC	Conventional methods (such as ELISA, PCR...)	Evaluation
Turnaround time	Minute-level to sub-hour detection	Several hours to 1–2 days	LoC is highly suitable for POCT
Sample and reagent consumption	Microliter to nanoliter sample volumes	Tens to hundreds of microliters	LoC significantly reduces the consumption of precious clinical specimens and costly reagents
Automation & operational complexity	Integrate sample preparation, reaction, washing, and detection on a single chip	Rely heavily on manual operation and technician expertise	LoC enables higher levels of automation, reduces human error, and improves reproducibility
Multiplexing & integration capability	Parallel detection of multiple biomarkers on a single chip through micro-compartment design	Typically single-analyte assays	Although LoC platforms inherently facilitate multiplexing by enabling compartmentalization into droplets or parallel microchannels, multiplexed detection within the same reaction space still faces challenges
Sensitivity & quantitative performance	Higher signal-to-noise ratios and lower LOD due to confined micro-reaction volumes	Offer well-established high sensitivity	Under certain specific conditions, such as extremely low abundance target detection, complex sample matrices, or environmental fluctuations, false positive/false negative issues may still occur in LoC
Portability & on-site application	Compact, energy-efficient, and compatible with smartphone-based or portable readout systems	Rely on bulky instruments, unsuitable for resource-limited settings	LoC is ideal for POCT, field sampling, and low-resource clinical environments. During the detection process, signals may be affected by various factors such as temperature, humidity, and electromagnetic interference, resulting in signal instability
Cost structure	Initial development and integration costs may be high, but large-scale clinical deployment can significantly reduce per-test cost	High capital equipment costs and moderate but consistent consumable costs	LoC can be mass-produced at low cost, depending on the material and fabrication



## 4. Conclusion and future vision

In conclusion, LoC technology represents a transformative paradigm in biomarker analysis, enabling ultrasensitive detection at the single-molecule level through integrated microfluidics and nano-biosensing. Its capability to process complex clinical samples within microliter volumes has revolutionized POCT diagnostics, which has greatly accelerated the timeliness and accessibility of diagnosis and promoted the optimization of personalized treatment strategies.<sup>179,180</sup>

Traditional biomarker testing requires multiple devices, professional operating environments, and lengthy processes (usually taking hours to days), making it difficult to meet the needs of emergency diagnosis. In contrast, LoC platforms integrate sample preparation, target enrichment, and signal amplification within a single device, improving analytical robustness by mitigating matrix interference and contributing to higher specificity with fewer false positives.<sup>181,182</sup> The high functionality of the LoC system in various biomarker detection has been demonstrated in various research studies or clinical practice. Although LoC offers notable benefits in improving the sensitivity, specificity, and throughput of molecule detection, it also has some limitations that need to be considered (Table 4). Below is an outline of the shortcomings alongside potential enhancements: 1) false positive/negative: under certain specific conditions, such as extremely low abundance target detection, complex sample matrices, or environmental fluctuations, false positive/false negative issues may still occur.<sup>183,184</sup> Stringent fluidic isolation, closed-cartridge designs, and antifouling surface chemistries, together with optimized affinity reagents, can markedly improve LoC performance by minimizing errors arising from non-specific binding and cross-contamination. 2) Reliability and standardization challenges: during the detection process, signals may be affected by various factors such as temperature, humidity, and electromagnetic interference, resulting in signal instability.<sup>185</sup> Additionally, variations between different chip batches or testing conducted by different operators can lead to inconsistencies in test outcomes, ultimately compromising repeatability and reproducibility. Standardized materials and surface treatments, process-controlled fabrication, and on-chip references with real-time QC and calibrated algorithms could improve the robustness and reproducibility of LoC assays.<sup>186</sup> 3) Multiplex detection limitations: although LoC platforms inherently facilitate multiplexing by enabling compartmentalization into droplets or parallel microchannels, multiplexed detection within the same reaction space still faces challenges. Signal interference can lead to spectral crosstalk and reduce detection accuracy, particularly in fluorescence-based assays.<sup>187</sup> Developing narrowband fluorescent probe materials, physically optimizing signal sources and acquisition systems, and logically optimizing signal processing and system design could promote robust protein and nucleic acid multiplex detection in LoC platforms. Further progress will also require more intelligent strategies for processing and interpreting LoC-derived data.

The growing sophistication of LoC platforms allows them to generate high-dimensional optical, electrochemical, and imaging datasets. However, conventional data processing methods now limit our ability to fully exploit their diagnostic potential. The convergence of LoC technologies with AI represents an emerging frontier.<sup>188</sup> AI, especially machine learning (ML) models, offers transformative capabilities by enabling automated signal interpretation, robust pattern recognition, real-time decision-making, and predictive analytics.<sup>189</sup> One of the most immediate benefits of integrating ML with LoC platforms lies in enhanced signal processing and noise reduction. Deep learning architectures, such as convolutional neural networks (CNNs) and autoencoders, have demonstrated superior performance in denoising fluorescence and electrochemical signals, identifying subtle biomarker-associated features that would otherwise be obscured by experimental variability.<sup>190,191</sup> These approaches can significantly improve sensitivity and lower the limit of detection, especially for assays targeting trace-level analytes in complex biological matrices. For image-based LoC systems, including those used in droplet microfluidics, single-cell capture, and extracellular vesicle profiling, ML-driven segmentation and classification are key to achieving higher throughput and reproducibility.<sup>192</sup> AI-driven biomarker interpretation represents another rapidly advancing domain. By integrating multi-parametric data including electrochemical currents, optical intensities, morphological patterns, and temporal trajectories, ML algorithms can power sophisticated clinical decision models.<sup>193</sup> These models enable risk stratification, multi-marker classification, and early disease prediction that surpass traditional threshold-based analyses.

Looking ahead, LoC technology is advancing towards greater automation and integration, driven by ongoing research and innovation. This progress promises to further reduce detection costs while enhancing efficiency and accuracy. Achieving these goals requires simplifying processes, improving specificity and sensitivity, strengthening quantitative capabilities, and overcoming multiplexing challenges. Multidisciplinary collaboration, advances in nanotechnology, and the integration of AI will be key drivers for next-generation LoC development. Overall, LoC technology demonstrates significant potential for diverse biomarker detection applications. As the technology continues to advance and mature, it is poised to overcome current limitations, becoming a more universal and reliable tool for molecular diagnostics. This evolution will enable it to address the growing demands of personalized medicine and digital healthcare ecosystems.

## Author contributions

T. Xu: investigation, writing – original draft, writing – review & editing. H. Bai: visualization, writing – review & editing. J. Hu: software, writing – original draft. L. Zhang: methodology. W. Zhuang: writing – review & editing. C. Zou: writing –

review & editing, resources. Y. Yao: conceptualization, writing – review & editing. W. Hu and J. Huang: supervision, writing – review & editing.

## Conflicts of interest

The authors declare no conflict of interest.

## Data availability

No primary research results, software or code have been included and no new data were generated or analysed as part of this review.

## Acknowledgements

This work was supported by the National Natural Science Foundation of China (32201090), the Fundamental Research Funds for the Central Universities (ZYGX2022YGRH002), and the Talents Program of Sichuan University (YJ202454).

## References

- M. N. Zhao, R. J. Wang, K. M. Yang, Y. H. Jiang, Y. C. Peng, Y. K. Li, Z. Zhang, J. X. Ding and S. J. Shi, *Acta Pharm. Sin. B*, 2023, **13**, 916–941, DOI: [10.1016/j.apsb.2022.10.019](https://doi.org/10.1016/j.apsb.2022.10.019).
- A. Campos-Carrillo, J. N. Weitzel, P. Sahoo, R. Rockne, J. V. Mokhnatkin, M. Murtaza, S. W. Gray, L. Goetz, A. Goel, N. Schork and T. P. Slavin, *Pharmacol. Ther.*, 2020, **207**, 107458, DOI: [10.1016/j.pharmthera.2019.107458](https://doi.org/10.1016/j.pharmthera.2019.107458).
- P. Johnson, Q. Zhou, D. Y. Dao and Y. M. D. Lo, *Nat. Rev. Gastroenterol. Hepatol.*, 2022, **19**, 670–681, DOI: [10.1038/s41575-022-00620-y](https://doi.org/10.1038/s41575-022-00620-y).
- M. Nikanjam, S. Kato and R. Kurzrock, *J. Hematol. Oncol.*, 2022, **15**, 131, DOI: [10.1186/s13045-022-01351-y](https://doi.org/10.1186/s13045-022-01351-y).
- Y. Lin, Y. Yang, Z. Li, L. Du, R. Shi, Q. Shi, X. Xu, G. Yin, F. Zhang, W. Huang, Y. Huang, G. Liao, Q. Liu, W. Li, H. Song and J. Huang, *Eur. J. Epidemiol.*, 2025, **40**, 1143–1159, DOI: [10.1007/s10654-025-01290-1](https://doi.org/10.1007/s10654-025-01290-1).
- D. M. Wang, S. G. He, X. H. Wang, Y. Q. Yan, J. Z. Liu, S. M. Wu, S. G. Liu, Y. Lei, M. Chen, L. Li, J. L. Zhang, L. W. Zhang, X. Hu, X. H. Zheng, J. W. Bai, Y. L. Zhang, Y. T. Zhang, M. X. Song and Y. G. Tang, *Nat. Biomed. Eng.*, 2020, **4**, 1150–1158, DOI: [10.1038/s41551-020-00655-z](https://doi.org/10.1038/s41551-020-00655-z).
- W. Gu, S. Miller and C. Y. Chiu, *Annu. Rev. Pathol.*, 2019, **14**, 319–338, DOI: [10.1146/annurev-pathmechdis-012418-012751](https://doi.org/10.1146/annurev-pathmechdis-012418-012751).
- T. Xu, J. Hu, C. Liu, H. Bai, L. Zhang, W. Zhuang, G. Wang, Z. Li, H. Lv, X. Sun and Y. Yao, *Biomed. Anal.*, 2025, **2**, 159–178, DOI: [10.1016/j.bioana.2025.11.004](https://doi.org/10.1016/j.bioana.2025.11.004).
- E. Samiei, M. Tabrizian and M. Hoorfar, *Lab Chip*, 2016, **16**, 2376–2396, DOI: [10.1039/c6lc00387g](https://doi.org/10.1039/c6lc00387g).
- T. Y. Zhang, F. Ding, Y. J. Yang, G. Z. Zhao, C. H. Zhang, R. M. Wang and X. W. Huang, *Biosensors*, 2022, **12**, 485, DOI: [10.3390/bios12070485](https://doi.org/10.3390/bios12070485).
- G. M. Whitesides, *Nature*, 2006, **442**, 368–373, DOI: [10.1038/nature05058](https://doi.org/10.1038/nature05058).
- E. K. Sackmann, A. L. Fulton and D. J. Beebe, *Nature*, 2014, **507**, 181–189, DOI: [10.1038/nature13118](https://doi.org/10.1038/nature13118).
- H. A. Stone, A. D. Stroock and A. Ajdari, *Annu. Rev. Fluid Mech.*, 2004, **36**, 381–411, DOI: [10.1146/annurev.fluid.36.050802.122124](https://doi.org/10.1146/annurev.fluid.36.050802.122124).
- S. Surappa, P. Multani, U. Parlatan, P. D. Sinawang, J. Kaifi, D. Akin and U. Demirci, *Lab Chip*, 2023, **23**, 2942–2958, DOI: [10.1039/d2lc01076c](https://doi.org/10.1039/d2lc01076c).
- G. Persichetti, I. A. Grimaldi, G. Testa and R. Bernini, *Lab Chip*, 2017, **17**, 2631–2639, DOI: [10.1039/c7lc00460e](https://doi.org/10.1039/c7lc00460e).
- S. Akgönüllü and A. Denizli, *J. Pharm. Biomed. Anal.*, 2023, **225**, 115213, DOI: [10.1016/j.jpba.2022.115213](https://doi.org/10.1016/j.jpba.2022.115213).
- J. Wang, D. Chen, W. Huang, N. Yang, Q. Yuan and Y. Yang, *Exploration*, 2023, **3**, 20210027, DOI: [10.1002/EXP.20210027](https://doi.org/10.1002/EXP.20210027).
- E. Mauri, S. M. Giannitelli, M. Trombetta and A. Rainer, *Gels*, 2021, **7**, 36, DOI: [10.3390/gels7020036](https://doi.org/10.3390/gels7020036).
- D. Wlodkowic and J. M. Cooper, *Anal. Bioanal. Chem.*, 2010, **398**, 193–209, DOI: [10.1007/s00216-010-3722-8](https://doi.org/10.1007/s00216-010-3722-8).
- S. J. Trietsch, T. Hankemeier and H. J. van der Linden, *Chemom. Intell. Lab. Syst.*, 2011, **108**, 64–75, DOI: [10.1016/j.chemolab.2011.03.005](https://doi.org/10.1016/j.chemolab.2011.03.005).
- J. D. Wu, M. L. Dong, S. Santos, C. Rigatto, Y. Liu and F. Lin, *Sensors*, 2017, **17**, 2934, DOI: [10.3390/s17122934](https://doi.org/10.3390/s17122934).
- P. P. Behera, N. Kumar, M. Kumari, S. Kumar, P. K. Mondal and R. K. Arun, *Sens. Diagn.*, 2023, **2**, 1437–1459, DOI: [10.1039/D3SD00170A](https://doi.org/10.1039/D3SD00170A).
- P. R. Li, S. K. Boilla, C. H. Wang, P. C. Lin, C. N. Kuo, T. H. Tsai and G. B. Lee, *Biosens. Bioelectron.*, 2024, **249**, 115931, DOI: [10.1016/j.bios.2023.115931](https://doi.org/10.1016/j.bios.2023.115931).
- V. T. Upaassana, S. Setty, H. Jang, S. Ghosh and C. Ahn, *Biomed. Microdevices*, 2025, **27**, 17, DOI: [10.1007/s10544-025-00733-6](https://doi.org/10.1007/s10544-025-00733-6).
- P. Balaji, D. Devasena, P. Rithick, T. Karthi, K. Rishmitha and R. Roopa, *2024 International Conference on Communication, Control, and Intelligent Systems (CCIS)*, 2024, pp. 1–6, DOI: [10.1109/ccis63231.2024.10931904](https://doi.org/10.1109/ccis63231.2024.10931904).
- H. Bai, J. Hu, T. Liu, L. Wan, C. Dong, D. Luo, F. Li, Z. Yuan, Y. Tang, T. Chen, S. Wang, H. Gou, Y. Zhou, B. Ying, J. Huang and W. W. Hu, *Lab Chip*, 2025, **25**, 1552–1564, DOI: [10.1039/d4lc00704b](https://doi.org/10.1039/d4lc00704b).
- M. Karmacharya, S. Kumar, C. Lee and Y.-K. Cho, *Biosens. Bioelectron.*, 2021, **194**, 113584, DOI: [10.1016/j.bios.2021.113584](https://doi.org/10.1016/j.bios.2021.113584).
- K. Khachornsakkul, F. J. Rybicki and S. Sonkusale, *Talanta*, 2023, **260**, 124538, DOI: [10.1016/j.talanta.2023.124538](https://doi.org/10.1016/j.talanta.2023.124538).
- G. Praveena, A. Jayachandran, S. M. Venkata and A. Asthana, *Colloids Surf., B*, 2025, **252**, 114675, DOI: [10.1016/j.colsurfb.2025.114675](https://doi.org/10.1016/j.colsurfb.2025.114675).
- R. Didarian and M. T. Azar, *Biomed. Microdevices*, 2025, **27**, DOI: [10.1007/s10544-025-00741-6](https://doi.org/10.1007/s10544-025-00741-6).
- K. Dashtian, F. Binabaji and R. Zare-Dorabei, *Anal. Chem.*, 2023, **95**, 16315–16326, DOI: [10.1021/acs.analchem.3c03516](https://doi.org/10.1021/acs.analchem.3c03516).
- G. Fu, X. Li, W. Wang and R. Hou, *Biosens. Bioelectron.*, 2020, **170**, 112646, DOI: [10.1016/j.bios.2020.112646](https://doi.org/10.1016/j.bios.2020.112646).
- M. A. Buttkewitz, C. Heuer and J. Bahnemann, *Curr. Opin. Biotechnol.*, 2023, **83**, 102978, DOI: [10.1016/j.copbio.2023.102978](https://doi.org/10.1016/j.copbio.2023.102978).

- 34 T. Shimada, Y. Ueda, Y. Baba and H. Yukawa, *Biosensors*, 2024, **14**, 340, DOI: [10.3390/bios14070340](https://doi.org/10.3390/bios14070340).
- 35 S. W. Chong, Y. Shen, S. Palomba and D. Vigolo, *Small*, 2025, **21**, e2407478, DOI: [10.1002/sml.202407478](https://doi.org/10.1002/sml.202407478).
- 36 I. Tzouvadaki, P. Gkoupidenis, S. Vassanelli, S. W. Wang and T. Prodromakis, *Adv. Mater.*, 2023, **35**, e2210035, DOI: [10.1002/adma.202210035](https://doi.org/10.1002/adma.202210035).
- 37 L. A. García-Hernández, E. Martínez-Martínez, D. Pazos-Solís, J. Aguado-Preciado, A. Dutt, A. U. Chávez-Ramírez, B. Korgel, A. Sharma and G. Oza, *Biosensors*, 2023, **13**, 439, DOI: [10.3390/bios13040439](https://doi.org/10.3390/bios13040439).
- 38 T. Sano, H. Zhang, R. Losakul and H. Schmidt, *Biosensors*, 2022, **12**, 501, DOI: [10.3390/bios12070501](https://doi.org/10.3390/bios12070501).
- 39 Y.-T. Tai, C.-Y. Wei and F.-H. Ko, *Biosens. Bioelectron.*, 2025, **271**, 117041, DOI: [10.1016/j.bios.2024.117041](https://doi.org/10.1016/j.bios.2024.117041).
- 40 T. T. Q. Nguyen, E. M. Lee, T. T. T. Dang, E. R. Kim, Y. Ko and M. B. Gu, *Biosens. Bioelectron.*, 2024, **251**, 116097, DOI: [10.1016/j.bios.2024.116097](https://doi.org/10.1016/j.bios.2024.116097).
- 41 B. Utzinger, D. D. Dixit and P. B. Lillehoj, *Lab Chip*, 2024, **24**, 3802–3809, DOI: [10.1039/d4lc00207e](https://doi.org/10.1039/d4lc00207e).
- 42 S. Kim, S. Kim, C. Ko, W. Lee and H. D. Kim, *Mater. Today Bio*, 2025, **32**, 101768, DOI: [10.1016/j.mtbio.2025.101768](https://doi.org/10.1016/j.mtbio.2025.101768).
- 43 Z. Liu, R. Chen, H. Wang, C. Wang, X. Zhang, Y. Yang, W. Pang, S. Ren, J. Yang, C. Yang, S. Li, H. Zhou and Z. Gao, *Biosens. Bioelectron.*, 2024, **263**, 116558, DOI: [10.1016/j.bios.2024.116558](https://doi.org/10.1016/j.bios.2024.116558).
- 44 H. Wang, L. Dong, L. Zhao, Y. Sun, R. Zhang and G. Shan, *Biosens. Bioelectron.*, 2025, **273**, 117162, DOI: [10.1016/j.bios.2025.117162](https://doi.org/10.1016/j.bios.2025.117162).
- 45 F. Leng, M. Zheng and C. Xu, *Exploration*, 2021, **1**, 20210109, DOI: [10.1002/EXP.20210109](https://doi.org/10.1002/EXP.20210109).
- 46 M. Yafia, O. Ymbern, A. O. Olanrewaju, A. Parandakh, A. Sohrabi Kashani, J. Renault, Z. Jin, G. Kim, A. Ng and D. Juncker, *Nature*, 2022, **605**, 464–469, DOI: [10.1038/s41586-022-04683-4](https://doi.org/10.1038/s41586-022-04683-4).
- 47 C. C. Chen, Y. H. Fu, S. S. Sparks, Z. Lyu, A. Pradhan, S. C. Ding, N. Boddeti, Y. Liu, Y. H. Lin, D. Du and K. Y. Qiu, *ACS Sens.*, 2024, **9**, 3212–3223, DOI: [10.1021/acssensors.4c00528](https://doi.org/10.1021/acssensors.4c00528).
- 48 M. Sharafeldin, K. Kadimisetty, K. S. Bhalerao, T. Q. Chen and J. F. Rusling, *Sensors*, 2020, **20**, 4514, DOI: [10.3390/s20164514](https://doi.org/10.3390/s20164514).
- 49 P. D. Sinawang, L. Fajs, K. Elouarzaki, J. Nugraha and R. S. Marks, *Sens. Actuators, B*, 2018, **259**, 354–363, DOI: [10.1016/j.snb.2017.12.043](https://doi.org/10.1016/j.snb.2017.12.043).
- 50 K. Hiniduma, K. S. Bhalerao, P. I. T. De Silva, T. Q. Chen and J. F. Rusling, *Micromachines*, 2023, **14**, 2187, DOI: [10.3390/mi14122187](https://doi.org/10.3390/mi14122187).
- 51 M. Calaon, G. Tosello, J. Garnaes and H. N. Hansen, *J. Micromech. Microeng.*, 2017, **27**, 105001, DOI: [10.1088/1361-6439/aa853f](https://doi.org/10.1088/1361-6439/aa853f).
- 52 K. Karimi, A. Fardoost, N. Mhatre, J. Rajan, D. Boisvert and M. Javanmard, *Micromachines*, 2024, **15**, 1274, DOI: [10.3390/mi15101274](https://doi.org/10.3390/mi15101274).
- 53 M. Matteucci, T. L. Christiansen, S. Tanzi, P. F. Ostergaard, S. T. Larsen and R. Taboryski, *Microelectron. Eng.*, 2013, **111**, 294–298, DOI: [10.1016/j.mee.2013.01.060](https://doi.org/10.1016/j.mee.2013.01.060).
- 54 M. Bhatt and P. Shende, *J. Mater. Chem. B*, 2022, **10**, 1176–1195, DOI: [10.1039/d1tb02455h](https://doi.org/10.1039/d1tb02455h).
- 55 I. Qavi, D. Sooriyaarachchi and G. Tan, *Manuf. Lett.*, 2023, **35**, 174–183, DOI: [10.1016/j.mfglet.2023.08.008](https://doi.org/10.1016/j.mfglet.2023.08.008).
- 56 L. Chen, G. Yang and F. Qu, *Talanta*, 2024, **268**, 125348, DOI: [10.1016/j.talanta.2023.125348](https://doi.org/10.1016/j.talanta.2023.125348).
- 57 M. Guma, S. Tiziani and G. S. Firestein, *Nat. Rev. Rheumatol.*, 2016, **12**, 269–281, DOI: [10.1038/nrrheum.2016.1](https://doi.org/10.1038/nrrheum.2016.1).
- 58 D. Shan, L. You, X. Wan, H. Yang, M. Zhao, S. Chen, W. Jiang, Q. Xu and Y. Yuan, *J. Affective Disord.*, 2023, **323**, 461–471, DOI: [10.1016/j.jad.2022.12.004](https://doi.org/10.1016/j.jad.2022.12.004).
- 59 K. A. Stringer, R. T. McKay, A. Karnovsky, B. Quémerais and P. Lacy, *Front. Immunol.*, 2016, **7**, 44, DOI: [10.3389/fimmu.2016.00044](https://doi.org/10.3389/fimmu.2016.00044).
- 60 I. Akyilmaz, D. Celebi-Birand, N. Y. Demir, D. Bas, C. Elbuken and M. Duman, *Lab Chip*, 2025, **25**, 1512–1520, DOI: [10.1039/d4lc00912f](https://doi.org/10.1039/d4lc00912f).
- 61 H.-B. Lee, M. Meeseepong, T. Q. Trung, B.-Y. Kim and N.-E. Lee, *Biosens. Bioelectron.*, 2020, **156**, 112133, DOI: [10.1016/j.bios.2020.112133](https://doi.org/10.1016/j.bios.2020.112133).
- 62 J. Narang, C. Singhal, A. Mathur, M. Khanuja, A. Varshney, K. Garg, T. Dahiya and C. S. Pundir, *Anal. Chim. Acta*, 2017, **980**, 50–57, DOI: [10.1016/j.aca.2017.05.006](https://doi.org/10.1016/j.aca.2017.05.006).
- 63 O. Korzhenko, P. Führer, V. Göldner, W. Olthuis, M. Odijk and U. Karst, *Anal. Chem.*, 2021, **93**, 12740–12747, DOI: [10.1021/acs.analchem.1c02791](https://doi.org/10.1021/acs.analchem.1c02791).
- 64 F. S. Mesquita, L. Abrami, M. E. Linder, S. X. Bamji, B. C. Dickinson and F. G. van der Goot, *Nat. Rev. Mol. Cell Biol.*, 2024, **25**, 488–509, DOI: [10.1038/s41580-024-00700-8](https://doi.org/10.1038/s41580-024-00700-8).
- 65 J. Wess, A.-B. Oteng, O. Rivera-Gonzalez, E. V. Gurevich and V. V. Gurevich, *Pharmacol. Rev.*, 2023, **75**, 854–884, DOI: [10.1124/pharmrev.121.000302](https://doi.org/10.1124/pharmrev.121.000302).
- 66 S. S. Pinho, I. Alves, J. Gaifem and G. A. Rabinovich, *Cell. Mol. Immunol.*, 2023, **20**, 1101–1113, DOI: [10.1038/s41423-023-01074-1](https://doi.org/10.1038/s41423-023-01074-1).
- 67 M. A. Saifi and I. C. Ho, *Philos. Trans. R. Soc., B*, 2023, **378**, 20220244, DOI: [10.1098/rstb.2022.0244](https://doi.org/10.1098/rstb.2022.0244).
- 68 C. Parra Bravo, S. A. Naguib and L. Gan, *Nat. Rev. Mol. Cell Biol.*, 2024, **25**, 845–864, DOI: [10.1038/s41580-024-00753-9](https://doi.org/10.1038/s41580-024-00753-9).
- 69 A. Dall'Agnesse, M. M. Zheng, S. Moreno, J. M. Platt, A. T. Hoang, D. Kannan, G. Dall'Agnesse, K. J. Overholt, I. Sagi, N. M. Hannett, H. Erb, O. Corradin, A. K. Chakraborty, T. I. Lee and R. A. Young, *Cell*, 2025, **188**, 207–221, DOI: [10.1016/j.cell.2024.10.051](https://doi.org/10.1016/j.cell.2024.10.051).
- 70 L. Niu, M. Thiele, P. E. Geyer, D. N. Rasmussen, H. E. Webel, A. Santos, R. Gupta, F. Meier, M. Strauss, M. Kjaergaard, K. Lindvig, S. Jacobsen, S. Rasmussen, T. Hansen, A. Krag and M. Mann, *Nat. Med.*, 2022, **28**, 1277–1287, DOI: [10.1038/s41591-022-01850-y](https://doi.org/10.1038/s41591-022-01850-y).
- 71 R. Ossenkoppele, R. van der Kant and O. Hansson, *Lancet Neurol.*, 2022, **21**, 726–734, DOI: [10.1016/S1474-4422\(22\)00168-5](https://doi.org/10.1016/S1474-4422(22)00168-5).
- 72 S. Spindel and K. E. Sapsford, *Sensors*, 2014, **14**, 22313–22341, DOI: [10.3390/s14122313](https://doi.org/10.3390/s14122313).
- 73 D. Li, Q. Xiong, D. Lu, Y. Chen, L. Liang and H. Duan, *Anal. Chim. Acta*, 2021, **1166**, 338567, DOI: [10.1016/j.aca.2021.338567](https://doi.org/10.1016/j.aca.2021.338567).

- 74 M. Ogrič, T. Švec, K. M. Poljšak, P. Žigon, A. Hočevar and S. Čučnik, *Clin. Chem. Lab. Med.*, 2024, **62**, 682–689, DOI: [10.1515/cclm-2023-0764](https://doi.org/10.1515/cclm-2023-0764).
- 75 J.-u. Shim, R. T. Ranasinghe, C. A. Smith, S. M. Ibrahim, F. Hollfelder, W. T. S. Huck, D. Klenerman and C. Abell, *ACS Nano*, 2013, **7**, 5955–5964, DOI: [10.1021/nn401661d](https://doi.org/10.1021/nn401661d).
- 76 A. Parandakh, O. Ymbern, W. Jogia, J. Renault, A. Ng and D. Juncker, *Lab Chip*, 2023, **23**, 1547–1560, DOI: [10.1039/d2lc00878e](https://doi.org/10.1039/d2lc00878e).
- 77 X. Shuqi, P. Jiangfei, D. Deshen, D. Zong, Y. Mengsu and Y. Changqing, *Chin. Chem. Lett.*, 2023, **34**, 107799, DOI: [10.1016/j.ccllet.2022.107799](https://doi.org/10.1016/j.ccllet.2022.107799).
- 78 L. H. Zhu, W. X. Fu, B. Y. Zhu, Q. Feng, X. D. Ying, S. Li, J. Chen, X. Y. Xie, C. Y. Pan, J. Liu, C. Chen, X. Chen and D. H. Zhu, *Talanta*, 2023, **262**, 124626, DOI: [10.1016/j.talanta.2023.124626](https://doi.org/10.1016/j.talanta.2023.124626).
- 79 Y. R. Liu, J. H. Li, T. Y. Wu, B. Y. Chen, J. P. Hu, Z. H. Xiao, H. R. Liang, S. H. He, H. Y. Hong, S. D. Chen and J. H. Zhou, *Sens. Actuators, B*, 2024, **418**, 136331, DOI: [10.1016/j.snb.2024.136331](https://doi.org/10.1016/j.snb.2024.136331).
- 80 S. J. Chen, S. Y. Lu, C. C. Tseng, K. H. Huang, T. L. Chen and L. M. Fu, *Biosensors*, 2024, **14**, 283, DOI: [10.3390/bios14060283](https://doi.org/10.3390/bios14060283).
- 81 N. Gobet, S. Ketterer and M. Meier, *PLoS One*, 2014, **9**, e112629, DOI: [10.1371/journal.pone.0112629](https://doi.org/10.1371/journal.pone.0112629).
- 82 W. L. Zhang, Z. Y. He, L. L. Yi, S. F. Mao, H. F. Li and J. M. Lin, *Biosens. Bioelectron.*, 2018, **102**, 652–660, DOI: [10.1016/j.bios.2017.12.017](https://doi.org/10.1016/j.bios.2017.12.017).
- 83 Y. L. Xianyu, J. Wu, Y. P. Chen, W. S. Zheng, M. X. Xie and X. Y. Jiang, *Angew. Chem., Int. Ed.*, 2018, **57**, 7503–7507, DOI: [10.1002/anie.201801815](https://doi.org/10.1002/anie.201801815).
- 84 G. Awiaz, J. Lin and A. Wu, *Exploration*, 2023, **3**, 20220072, DOI: [10.1002/EXP.20220072](https://doi.org/10.1002/EXP.20220072).
- 85 V. T. Upaassana, S. Ghosh, A. Chakraborty, M. E. Birch, P. Joseph, J. Han, B. K. Ku and C. H. Ahn, *Anal. Chem.*, 2019, **91**, 6652–6660, DOI: [10.1021/acs.analchem.9b00582](https://doi.org/10.1021/acs.analchem.9b00582).
- 86 A. Chiadò, G. Palmara, A. Chiappone, C. Tanzanu, C. F. Pirri, I. Roppolo and F. Frascella, *Lab Chip*, 2020, **20**, 665–674, DOI: [10.1039/c9lc01108k](https://doi.org/10.1039/c9lc01108k).
- 87 F. Weihs, M. Gel, J. Wang, A. Anderson, S. Trowell and H. Dacres, *Biosens. Bioelectron.*, 2020, **158**, 112162, DOI: [10.1016/j.bios.2020.112162](https://doi.org/10.1016/j.bios.2020.112162).
- 88 S. P. Ning, H. C. Chang, K. C. Fan, P. Y. Hsiao, C. H. Feng, D. Shoemaker and R. T. Chen, *Appl. Phys. Rev.*, 2023, **10**, 021410, DOI: [10.1063/5.0146079](https://doi.org/10.1063/5.0146079).
- 89 X. W. Cao, S. J. Ge, M. Chen, H. Y. Mao and Y. Wang, *ACS Appl. Mater. Interfaces*, 2023, **15**, 21830–21842, DOI: [10.1021/acsami.3c00103](https://doi.org/10.1021/acsami.3c00103).
- 90 N. H. Bhuiyan and J. S. Shim, *Biosens. Bioelectron.*, 2024, **244**, 115791, DOI: [10.1016/j.bios.2023.115791](https://doi.org/10.1016/j.bios.2023.115791).
- 91 Y. W. Zhuang, F. Lu, X. Y. Wang, J. Yao, Y. Wan, S. C. Qin, X. W. Cao and J. X. Sheng, *Talanta*, 2025, **294**, 128190, DOI: [10.1016/j.talanta.2025.128190](https://doi.org/10.1016/j.talanta.2025.128190).
- 92 X. J. Liu, J. C. Guo, Y. Li, B. Wang, S. K. Yang, W. J. Chen, X. G. Wu, J. H. Guo and X. Ma, *J. Mater. Chem. B*, 2021, **9**, 8378–8388, DOI: [10.1039/d1tb01299a](https://doi.org/10.1039/d1tb01299a).
- 93 S. J. Ge, G. Y. Chen, J. L. Deng, Y. X. Gu, Y. Mao, X. Y. Zhou and G. Li, *Anal. Chim. Acta*, 2023, **1247**, 340890, DOI: [10.1016/j.aca.2023.340890](https://doi.org/10.1016/j.aca.2023.340890).
- 94 P. D. Gomes, M. Hin-Chu, J. J. S. Rickard and P. G. Oppenheimer, *Adv. Sci.*, 2024, **11**, e2306068, DOI: [10.1002/adv.202306068](https://doi.org/10.1002/adv.202306068).
- 95 C. W. Lin, L. Y. Chen, Y. C. Huang, P. Kumar, Y. Z. Guo, C. H. Wu, L. M. Wang and K. L. Chen, *ACS Sens.*, 2024, **9**, 305–314, DOI: [10.1021/acssensors.3c02007](https://doi.org/10.1021/acssensors.3c02007).
- 96 P. P. Niu, J. F. Jiang, K. Liu, X. Zhou, S. Wang, T. H. Xu, T. Wang, Y. L. Li, Q. Yang and T. G. Liu, *Biosens. Bioelectron.*, 2024, **248**, 115970, DOI: [10.1016/j.bios.2023.115970](https://doi.org/10.1016/j.bios.2023.115970).
- 97 M. Chen, S. Yao, Y. Yang, F. Jiang, Y. Yang, Y. Gu, Z. Wang, X. Cao and W. Wei, *Microchem. J.*, 2023, **193**, 109106, DOI: [10.1016/j.microc.2023.109106](https://doi.org/10.1016/j.microc.2023.109106).
- 98 M. Ignatiadis, G. W. Sledge and S. S. Jeffrey, *Nat. Rev. Clin. Oncol.*, 2021, **18**, 297–312, DOI: [10.1038/s41571-020-00457-x](https://doi.org/10.1038/s41571-020-00457-x).
- 99 J. Wang, J. Huang, Y. Hu, Q. Guo, S. Zhang, J. Tian, Y. Niu, L. Ji, Y. Xu, P. Tang, Y. He, Y. Wang, S. Zhang, H. Yang, K. Kang, X. Chen, X. Li, M. Yang and D. Gou, *Nat. Commun.*, 2024, **15**, 156, DOI: [10.1038/s41467-023-44461-y](https://doi.org/10.1038/s41467-023-44461-y).
- 100 A. Zviran, R. C. Schulman, M. Shah, S. T. K. Hill, S. Deochand, C. C. Khamnei, D. Maloney, K. Patel, W. Liao, A. J. Widman, P. Wong, M. K. Callahan, G. Ha, S. Reed, D. Rotem, D. Frederick, T. Sharova, B. Miao, T. Kim, G. Gydush, J. Rhoades, K. Y. Huang, N. D. Omans, P. O. Bolan, A. H. Lipsky, C. Ang, M. Malbari, C. F. Spinelli, S. Kazancioglu, A. M. Runnels, S. Fennessey, C. Stolte, F. Gaiti, G. G. Inghirami, V. Adalsteinsson, B. Houck-Loomis, J. Ishii, J. D. Wolchok, G. Boland, N. Robine, N. K. Altorki and D. A. Landau, *Nat. Med.*, 2020, **26**, 1114–1124, DOI: [10.1038/s41591-020-0915-3](https://doi.org/10.1038/s41591-020-0915-3).
- 101 D. C. Bruhm, N. A. Vulpescu, Z. H. Foda, J. Phallen, R. B. Scharpf and V. E. Velculescu, *Nat. Rev. Cancer*, 2025, **25**, 341–358, DOI: [10.1038/s41568-025-00795-x](https://doi.org/10.1038/s41568-025-00795-x).
- 102 R. Paul, E. Ostermann and Q. Wei, *Biosens. Bioelectron.*, 2020, **169**, 112592, DOI: [10.1016/j.bios.2020.112592](https://doi.org/10.1016/j.bios.2020.112592).
- 103 G. Gharib, İ. Bütün, Z. Munganlı, G. Kozalak, İ. Namlı, S. S. Sarraf, V. E. Ahmadi, E. Toyran, A. J. van Wijnen and A. Koşar, *Biosensors*, 2022, **12**, 1023, DOI: [10.3390/bios12111023](https://doi.org/10.3390/bios12111023).
- 104 G. Kaur, M. Tintelott, M. Suranglikar, A. Masurier, X.-T. Vu, G. Gines, Y. Rondelez, S. Ingebrandt, Y. Coffinier, V. Pachauri and A. Vlandas, *Biosens. Bioelectron.*, 2024, **257**, 116311, DOI: [10.1016/j.bios.2024.116311](https://doi.org/10.1016/j.bios.2024.116311).
- 105 Q. Ruan, F. Zou, Y. Wang, Y. Zhang, X. Xu, X. Lin, T. Tian, H. Zhang, L. Zhou, Z. Zhu and C. Yang, *ACS Appl. Mater. Interfaces*, 2021, **13**, 8042–8048, DOI: [10.1021/acsami.0c21995](https://doi.org/10.1021/acsami.0c21995).
- 106 D. X. Zhang, R. X. Gao, S. L. Huang, Y. L. Huang, J. B. Zhang, X. S. Su, S. Y. Zhang, S. X. Ge, J. Zhang and N. S. Xia, *Sens. Actuators, B*, 2023, **390**, 133939, DOI: [10.1016/j.snb.2023.133939](https://doi.org/10.1016/j.snb.2023.133939).
- 107 M. L. Cunha, S. S. da Silva, M. C. Stracke, D. L. Zanette, M. N. Aoki and L. Blanes, *Anal. Chem.*, 2022, **94**, 41–58, DOI: [10.1021/acs.analchem.1c04460](https://doi.org/10.1021/acs.analchem.1c04460).



- 108 Y. X. Lu, J. B. Zhang, X. N. Lu and Q. Liu, *Trends Food Sci. Technol.*, 2024, **148**, 104482, DOI: [10.1016/j.tifs.2024.104482](https://doi.org/10.1016/j.tifs.2024.104482).
- 109 K. Kojima, K. M. Juma, S. Akagi, K. Hayashi, T. Takita, C. K. O'Sullivan, S. Fujiwara, Y. Nakura, I. Yanagihara and K. Yasukawa, *J. Biosci. Bioeng.*, 2021, **131**, 219–224, DOI: [10.1016/j.jbiosc.2020.10.001](https://doi.org/10.1016/j.jbiosc.2020.10.001).
- 110 Y. X. Chen, Y. X. Hu and X. A. Lu, *ACS Sens.*, 2023, **8**, 2331–2339, DOI: [10.1021/acssensors.3c00387](https://doi.org/10.1021/acssensors.3c00387).
- 111 L.-S. Yu, J. Rodriguez-Manzano, N. Moser, A. Moniri, K. Malpartida-Cardenas, N. Miscourides, T. Sewell, T. Kochina, A. Brackin, J. Rhodes, A. H. Holmes, M. C. Fisher and P. Georgiou, *J. Clin. Microbiol.*, 2020, **58**, e00843-20, DOI: [10.1128/JCM.00843-20](https://doi.org/10.1128/JCM.00843-20).
- 112 J. Zhang, L. Xu, Z. Sheng, J. Zheng, W. Chen, Q. Hu and F. Shen, *ACS Sens.*, 2024, **9**, 646–653, DOI: [10.1021/acssensors.3c01727](https://doi.org/10.1021/acssensors.3c01727).
- 113 T. Xu, Y. Zhang, S. Li, C. Dai, H. Wei, D. Chen, Y. Zhao, H. Liu, D. Li, P. Chen, B.-F. Liu and Y. Tian, *Adv. Sci.*, 2025, **12**, e2414918, DOI: [10.1002/advs.202414918](https://doi.org/10.1002/advs.202414918).
- 114 T. L. Dangerfield, I. Paik, S. Bhadra, K. A. Johnson and A. D. Ellington, *Nucleic Acids Res.*, 2022, **51**, 488–499, DOI: [10.1093/nar/gkac1221.108](https://doi.org/10.1093/nar/gkac1221.108).
- 115 F. Garbarino, G. A. S. Minero, G. Rizzi, J. Fock and M. F. Hansen, *Biosens. Bioelectron.*, 2019, **142**, 111485, DOI: [10.1016/j.bios.2019.111485](https://doi.org/10.1016/j.bios.2019.111485).
- 116 P. Rodriguez-Mateos, B. Ngamsom, C. Walter, C. E. Dyer, J. Gitaka, A. Iles and N. Pamme, *Anal. Chim. Acta*, 2021, **1177**, 338758, DOI: [10.1016/j.aca.2021.338758](https://doi.org/10.1016/j.aca.2021.338758).
- 117 Y. X. Chen, Y. X. Hu and X. A. Lu, *ACS Sens.*, 2023, **8**, 2331–2339, DOI: [10.1021/acssensors.3c00387](https://doi.org/10.1021/acssensors.3c00387).
- 118 Y. X. Chen, Y. X. Hu and X. A. Lu, *Appl. Environ. Microbiol.*, 2023, **89**, e0069523, DOI: [10.1128/aem.00695-23](https://doi.org/10.1128/aem.00695-23).
- 119 Z. W. Li, T. C. Li, F. Costantini, N. Lovecchio, Y. Chang, D. Caputo and X. X. Duan, *Anal. Chem.*, 2024, **96**, 11572–11580, DOI: [10.1021/acs.analchem.4c02447](https://doi.org/10.1021/acs.analchem.4c02447).
- 120 Y. X. Lu, M. Z. Hua, Y. H. Luo, X. N. Lu and Q. Liu, *Appl. Environ. Microbiol.*, 2024, **90**, e0120824, DOI: [10.1128/aem.01208-24](https://doi.org/10.1128/aem.01208-24).
- 121 I. Bachmann, O. Behrmann, M. Klingenberg-Ernst, M. Rupnik, F. T. Hufert, G. Dame and M. Weidmann, *Anal. Chem.*, 2024, **96**, 3267–3275, DOI: [10.1021/acs.analchem.3c02985](https://doi.org/10.1021/acs.analchem.3c02985).
- 122 L. G. Liang, P. Wang, J. M. Fu, L. W. Zhu, L. F. Cheng, F. M. Liu, N. P. Wu, L. H. Xu, H. P. Yao and H. B. Wu, *Poult. Sci.*, 2025, **104**, 105463, DOI: [10.1016/j.psj.2025.105463](https://doi.org/10.1016/j.psj.2025.105463).
- 123 Y. H. Huang and S. Jiang, *Environ. Sci. Technol.*, 2025, **59**, 3088–3097, DOI: [10.1021/acs.est.4c13718](https://doi.org/10.1021/acs.est.4c13718).
- 124 C. Casas-Arozamena, A. Vilar, J. Cueva, E. Arias, V. Sampayo, E. Diaz, S. S. Oltra, C. P. Moiola, S. Cabrera, A. Cortegoso, T. Curiel, A. Abalo, M. Pamies Serrano, S. Domingo, P. Padilla-Iserte, M. Arnaez de la Cruz, A. Hernández, V. García-Pineda, J. Ruiz-Bañobre, R. López, X. Matias-Guiu, E. Colás, A. Gil-Moreno, M. Abal, G. Moreno-Bueno and L. Muinelo-Romay, *J. Exp. Clin. Cancer Res.*, 2024, **43**, 264, DOI: [10.1186/s13046-024-03158-w](https://doi.org/10.1186/s13046-024-03158-w).
- 125 C. M. Ackerman, C. Myhrvold, S. G. Thakku, C. A. Freije, H. C. Metsky, D. K. Yang, S. H. Ye, C. K. Boehm, T.-S. F. Kosoko-Thoroddsen, J. Kehe, T. G. Nguyen, A. Carter, A. Kulesa, J. R. Barnes, V. G. Dugan, D. T. Hung, P. C. Blainey and P. C. Sabeti, *Nature*, 2020, **582**, 277–282, DOI: [10.1038/s41586-020-2279-8](https://doi.org/10.1038/s41586-020-2279-8).
- 126 H. Lin, W. Yu, K. A. Sabet, M. Bogumil, Y. Zhao, J. Hambalek, S. Lin, S. Chandrasekaran, O. Garner, D. Di Carlo and S. Emaminejad, *Nature*, 2022, **611**, 570–577, DOI: [10.1038/s41586-022-05408-3](https://doi.org/10.1038/s41586-022-05408-3).
- 127 N. L. Welch, M. Zhu, C. Hua, J. Weller, M. E. Mirhashemi, T. G. Nguyen, S. Mantena, M. R. Bauer, B. M. Shaw, C. M. Ackerman, S. G. Thakku, M. W. Tse, J. Kehe, M.-M. Uwera, J. S. Eversley, D. A. Bielwaski, G. McGrath, J. Braidt, J. Johnson, F. Cerrato, G. K. Moreno, L. A. Krasilnikova, B. A. Petros, G. L. Gionet, E. King, R. C. Huard, S. K. Jalbert, M. L. Cleary, N. A. Fitzgerald, S. B. Gabriel, G. R. Gallagher, S. C. Smole, L. C. Madoff, C. M. Brown, M. W. Keller, M. M. Wilson, M. K. Kirby, J. R. Barnes, D. J. Park, K. J. Siddle, C. T. Happi, D. T. Hung, M. Springer, B. L. MacInnis, J. E. Lemieux, E. Rosenberg, J. A. Branda, P. C. Blainey, P. C. Sabeti and C. Myhrvold, *Nat. Med.*, 2022, **28**, 1083–1094, DOI: [10.1038/s41591-022-01734-1](https://doi.org/10.1038/s41591-022-01734-1).
- 128 G. Bhattacharjee, R. Maurya, K. J. Alzahrani, N. Gohil, N. L. Lam and V. Singh, *Prog. Mol. Biol. Transl. Sci.*, 2022, **187**, 241–248, DOI: [10.1016/bs.pmbts.2021.07.024](https://doi.org/10.1016/bs.pmbts.2021.07.024).
- 129 J. Hu, H. Bai, L. Wang, J. Li, Y. Shen, L. Zhang, J. Tang, M. Wang, Q. Liu, J. Zhou, Y. Zhou, J. Xiang, H. Tang, Z. Zhang, J. Huang, B. Ying, W. Li and W. Hu, *Sens. Actuators, B*, 2024, **411**, 135740, DOI: [10.1016/j.snb.2024.135740](https://doi.org/10.1016/j.snb.2024.135740).
- 130 H. Bai, Y. Liu, L. Gao, T. Wang, X. Zhang, J. Hu, L. Ding, Y. Zhang, Q. Wang, L. Wang, J. Li, Z. Zhang, Y. Wang, C. Shen, B. Ying, X. Niu and W. Hu, *Biosens. Bioelectron.*, 2024, **248**, 115968, DOI: [10.1016/j.bios.2023.115968](https://doi.org/10.1016/j.bios.2023.115968).
- 131 L. Liang, Y. Zhang, C. Li, Y. Liao, G. Wang, J. Xu, Y. Li, G. Yuan, Y. Sun, R. Zhang, X. Li, W. Nian, J. Zhao, Y. Zhang, X. Zhu, X. Wen, S. Cai, N. Li and L. Wu, *EBioMedicine*, 2022, **83**, 104222, DOI: [10.1016/j.ebiom.2022.104222](https://doi.org/10.1016/j.ebiom.2022.104222).
- 132 S. Heeke, C. M. Gay, M. R. Estecio, H. Tran, B. B. Morris, B. Zhang, X. Tang, M. G. Raso, P. Rocha, S. Lai, E. Arriola, P. Hofman, V. Hofman, P. Kopparapu, C. M. Lovly, K. Concannon, L. G. De Sousa, W. E. Lewis, K. Kondo, X. Hu, A. Tanimoto, N. I. Vokes, M. B. Nilsson, A. Stewart, M. Jansen, I. Horváth, M. Gaga, V. Panagoulas, Y. Raviv, D. Frumkin, A. Wasserstrom, A. Shuali, C. A. Schnabel, Y. Xi, L. Diao, Q. Wang, J. Zhang, P. Van Loo, J. Wang, I. I. Wistuba, L. A. Byers and J. V. Heymach, *Cancer Cell*, 2024, **42**, 225–237, DOI: [10.1016/j.ccell.2024.01.001](https://doi.org/10.1016/j.ccell.2024.01.001).
- 133 K. M. Koo, S. Dey and M. Trau, *ACS Sens.*, 2018, **3**, 2597–2603, DOI: [10.1021/acssensors.8b01011](https://doi.org/10.1021/acssensors.8b01011).
- 134 S. K. Kotla, P. V. Kadambi, A. R. Hendricks and R. Rojas, *Nephrol., Dial., Transplant.*, 2021, **36**, 587–593, DOI: [10.1093/ndt/gfz273](https://doi.org/10.1093/ndt/gfz273).
- 135 L. Xu, H. J. Qu, D. G. Alonso, Z. Q. Yu, Y. Yu, Y. J. Shi, C. L. Hu, T. Y. Zhu, N. N. Wu and F. Shen, *Biosens. Bioelectron.*, 2021, **175**, 112908, DOI: [10.1016/j.bios.2020.112908](https://doi.org/10.1016/j.bios.2020.112908).

- 136 D. Chu, Y.-H. Oh, H. Sung, D.-H. Ko, H.-B. Oh and S.-H. Hwang, *J. Med. Virol.*, 2024, **96**, e29919, DOI: [10.1002/jmv.29919](https://doi.org/10.1002/jmv.29919).
- 137 F. Costantini, N. Lovecchio, M. Nandimandalam, A. Mangli, F. Faggioli, M. Biasin, C. Manetti, P. F. Roversi, A. Nascetti, G. de Cesare and D. Caputo, *Biosensors*, 2023, **13**, 544, DOI: [10.3390/bios13050544](https://doi.org/10.3390/bios13050544).
- 138 T. L. Quyen, A. C. Vinayaka, M. Golabi, T. Nguyen, H. Van Ngoc, D. D. Bang and A. Wolff, *ACS Sens.*, 2022, **7**, 3343–3351, DOI: [10.1021/acssensors.2c01337](https://doi.org/10.1021/acssensors.2c01337).
- 139 G. Xing, Y. Shang, X. Wang, Z. Wu, Q. Zhang, J. Ai, Q. Pu and L. Lin, *Chin. Chem. Lett.*, 2024, **35**, 109491, DOI: [10.1016/j.ccllet.2024.109491](https://doi.org/10.1016/j.ccllet.2024.109491).
- 140 T. AbdElFatah, M. Jalali, S. G. Yedire, I. I. Hosseini, C. Del Real Mata, H. Khan, S. V. Hamidi, O. Jeanne, R. Siavash Moakhar, M. McLean, D. Patel, Z. Wang, G. McKay, M. Yousefi, D. Nguyen, S. M. Vidal, C. Liang and S. Mahshid, *Nat. Nanotechnol.*, 2023, **18**, 922–932, DOI: [10.1038/s41565-023-01384-5](https://doi.org/10.1038/s41565-023-01384-5).
- 141 F. Ahmadi, F. Z. Zanganeh, I. A. Tehrani, S. Shoae, H. Choobin, A. Bozorg and M. Taghipoor, *Diagn. Microbiol. Infect. Dis.*, 2024, **109**, 116325, DOI: [10.1016/j.diagmicrobio.2024.116325](https://doi.org/10.1016/j.diagmicrobio.2024.116325).
- 142 E. Rosàs-Canyelles, A. J. Modzelewski, A. E. Gomez Martinez, A. Geldert, A. Gopal, L. He and A. E. Herr, *Lab Chip*, 2021, **21**, 2427–2436, DOI: [10.1039/d1lc00073j](https://doi.org/10.1039/d1lc00073j).
- 143 V. Iyer, Z. Yang, J. Ko, R. Weissleder and D. Issadore, *Lab Chip*, 2022, **22**, 3110–3121, DOI: [10.1039/d2lc00024e](https://doi.org/10.1039/d2lc00024e).
- 144 S. L. Hong, M. F. Zhang, X. Wang, H. H. Liu, N. A. Zhang, M. Tang and W. Li, *Crit. Rev. Anal. Chem.*, 2024, **54**, 2658–2669, DOI: [10.1080/10408347.2023.2195940](https://doi.org/10.1080/10408347.2023.2195940).
- 145 D. Najjar, J. Rainbow, S. S. Timilsina, P. Jolly, H. de Puig, M. Yafia, N. Durr, H. Sallum, G. Alter, J. Z. Li, X. G. Yu, D. R. Walt, J. A. Paradiso, P. Estrela, J. J. Collins and D. E. Ingber, *Nat. Biomed. Eng.*, 2022, **6**, 968–978, DOI: [10.1038/s41551-022-00919-w](https://doi.org/10.1038/s41551-022-00919-w).
- 146 J. Qian, J. Xia, S. Chiang, J. F. Liu, K. Li, F. Li, F. Wei, M. Aziz, Y. Kim, V. Go, J. Morizio, R. Zhong, Y. He, K. Yang, O. O. Yang, D. T. W. Wong, L. P. Lee and T. J. Huang, *Sci. Adv.*, 2025, **11**, eadt5464, DOI: [10.1126/sciadv.adt5464](https://doi.org/10.1126/sciadv.adt5464).
- 147 M. H. Kafshgari and O. Hayden, *Nano Sel.*, 2023, **4**, 1–47, DOI: [10.1002/nano.202200158](https://doi.org/10.1002/nano.202200158).
- 148 D. Dzikonski, R. Zamboni, A. Bandyopadhyay, D. Paul, R. Wedlich-Söldner, C. Denz and J. Imbrock, *Biomed. Microdevices*, 2025, **27**, 12, DOI: [10.1007/s10544-025-00739-0](https://doi.org/10.1007/s10544-025-00739-0).
- 149 P. Gupta, A. Mohan, A. Mishra, A. Nair, N. Chowdhury, D. Balekai, K. Rai, A. Prabhakar and T. Saiyed, *Microsyst. Nanoeng.*, 2024, **10**, 35, DOI: [10.1038/s41378-024-00665-w](https://doi.org/10.1038/s41378-024-00665-w).
- 150 V. Yaghoubi Naei, P. Bordhan, F. Mirakhorli, M. Khorrami, J. Shrestha, H. Nazari, A. Kulasinghe and M. Ebrahimi Warkiani, *Ther. Adv. Med. Oncol.*, 2023, **15**, 17588359231192401, DOI: [10.1177/17588359231192401](https://doi.org/10.1177/17588359231192401).
- 151 J. Zhuang, L. Xia, Z. Zou, J. Yin, N. Lin and Y. Mu, *Biosens. Bioelectron.*, 2022, **217**, 114715, DOI: [10.1016/j.bios.2022.114715](https://doi.org/10.1016/j.bios.2022.114715).
- 152 W. Feng, K. Xuemin, L. Yixuan, W. Shuli, C. Zhong and H. Xu, *Chin. Chem. Lett.*, 2024, **35**, 109754, DOI: [10.1016/j.ccllet.2024.109754](https://doi.org/10.1016/j.ccllet.2024.109754).
- 153 J. L. Ma, Y. Chen, J. Ren, T. P. Zhou, Z. L. Wang, C. Li, L. Qiu, T. Gao, P. Ding, Z. X. Ding, L. Ou, J. Wang, J. N. Xu, Z. R. Zhou, C. X. Jia, N. Sun, R. J. Pei and W. P. Zhu, *ACS Sens.*, 2023, **8**, 3744–3753, DOI: [10.1021/acssensors.3c01063](https://doi.org/10.1021/acssensors.3c01063).
- 154 I. Namli, S. Seyedmirzaei Sarraf, A. Sheibani Aghdam, G. Celebi Torabfam, O. Kutlu, S. Cetinel, M. Ghorbani and A. Koşar, *ACS Appl. Mater. Interfaces*, 2022, **14**, 40688–40697, DOI: [10.1021/acsami.2c12356](https://doi.org/10.1021/acsami.2c12356).
- 155 M. A. Kumar, S. K. Baba, H. Q. Sadida, S. A. Marzooqi, J. Jerobin, F. H. Altemani, N. Algehainy, M. A. Alanazi, A.-B. Abou-Samra, R. Kumar, A. S. Al-Shabeeb Akil, M. A. Macha, R. Mir and A. A. Bhat, *Signal Transduction Targeted Ther.*, 2024, **9**, 27, DOI: [10.1038/s41392-024-01735-1](https://doi.org/10.1038/s41392-024-01735-1).
- 156 R. P. Carney, R. R. Mizenko, B. T. Bozkurt, N. Lowe, T. Henson, A. Arizzi, A. Wang, C. Tan and S. C. George, *Nat. Nanotechnol.*, 2025, **20**, 14–25, DOI: [10.1038/s41565-024-01774-3](https://doi.org/10.1038/s41565-024-01774-3).
- 157 K.-S. Park, C. Lässer and J. Lötvall, *Physiol. Rev.*, 2025, **105**, 1733–1821, DOI: [10.1152/physrev.00032.2024](https://doi.org/10.1152/physrev.00032.2024).
- 158 F. Fabbiano, J. Corsi, E. Gurrieri, C. Trevisan, M. Notarangelo and V. G. D'Agostino, *J. Extracell. Vesicles*, 2020, **10**, e12043, DOI: [10.1002/jev2.12043](https://doi.org/10.1002/jev2.12043).
- 159 B. Yin, J. Ni, C. E. Witherel, M. Yang, J. A. Burdick, C. Wen and S. H. D. Wong, *Theranostics*, 2022, **12**, 207–231, DOI: [10.7150/thno.62708](https://doi.org/10.7150/thno.62708).
- 160 R. Upadhyaya, W. Zingg, S. Shetty and A. K. Shetty, *J. Controlled Release*, 2020, **323**, 225–239, DOI: [10.1016/j.jconrel.2020.04.017](https://doi.org/10.1016/j.jconrel.2020.04.017).
- 161 E. Serrano-Pertierra, M. Oliveira-Rodríguez, M. Matos, G. Gutiérrez, A. Moyano, M. Salvador, M. Rivas and M. C. Blanco-López, *Biomolecules*, 2020, **10**, 824, DOI: [10.3390/biom10060824](https://doi.org/10.3390/biom10060824).
- 162 C. Zhang, C. Qin, S. Dewanjee, H. Bhattacharya, P. Chakraborty, N. K. Jha, M. Gangopadhyay, S. K. Jha and Q. Liu, *Mol. Cancer*, 2024, **23**, 18, DOI: [10.1186/s12943-024-01932-0](https://doi.org/10.1186/s12943-024-01932-0).
- 163 V. Bahrambeigi, J. J. Lee, V. Branchi, K. I. Rajapakshe, Z. Xu, N. Kui, J. T. Henry, W. Kun, B. M. Stephens, S. Dhebat, M. W. Hurd, R. Sun, P. Yang, E. Ruppini, W. Wang, S. Kopetz, A. Maitra and P. A. Guerrero, *Cancer Res.*, 2024, **84**, 1719–1732, DOI: [10.1158/0008-5472.CAN-23-4070](https://doi.org/10.1158/0008-5472.CAN-23-4070).
- 164 R. C. C. de Freitas, R. D. C. Hirata, M. H. Hirata and E. Aikawa, *Biomolecules*, 2021, **11**, 388, DOI: [10.3390/biom11030388](https://doi.org/10.3390/biom11030388).
- 165 K. Brennan, K. Martin, S. P. FitzGerald, J. O'Sullivan, Y. Wu, A. Blanco, C. Richardson and M. M. Mc Gee, *Sci. Rep.*, 2020, **10**, 1039, DOI: [10.1038/s41598-020-57497-7](https://doi.org/10.1038/s41598-020-57497-7).
- 166 N. Karimi, A. Cvjetkovic, S. C. Jang, R. Crescitelli, M. A. Hosseinpour Feizi, R. Nieuwland, J. Lötvall and C. Lässer, *Cell. Mol. Life Sci.*, 2018, **75**, 2873–2886, DOI: [10.1007/s00018-018-2773-4](https://doi.org/10.1007/s00018-018-2773-4).
- 167 J. S. Del Río, Y. Son, J. Park, V. Sunkara and Y. K. Cho, *Langmuir*, 2024, **40**, 25772–25784, DOI: [10.1021/acs.langmuir.4c02098](https://doi.org/10.1021/acs.langmuir.4c02098).

- 168 C. X. Ji, M. F. Zhang, X. Wang, H. H. Liu, M. H. Wu, W. Li, Z. L. Yu and S. L. Hong, *Sens. Actuators, B*, 2025, **423**, 136786, DOI: [10.1016/j.snb.2024.136786](https://doi.org/10.1016/j.snb.2024.136786).
- 169 X. N. Guo, F. Hu, Z. Yong, S. H. Zhao, Y. Wan, B. Q. Wang and N. C. Peng, *Anal. Chem.*, 2024, **96**, 7212–7219, DOI: [10.1021/acs.analchem.4c00795](https://doi.org/10.1021/acs.analchem.4c00795).
- 170 M. Lan, Z. Ren, C. Cheng, G. Y. Li and F. Yang, *Biosens. Bioelectron.*, 2024, **259**, 116382, DOI: [10.1016/j.bios.2024.116382](https://doi.org/10.1016/j.bios.2024.116382).
- 171 X. Chen, J. Tang, Y. Zhao, R. Wang, S. Sang, F. Yu and Y. Xing, *Biosens. Bioelectron.*, 2025, **267**, 116724, DOI: [10.1016/j.bios.2024.116724](https://doi.org/10.1016/j.bios.2024.116724).
- 172 D. Yu, J. Gu, J. Zhang, M. Wang, R. Ji, C. Feng, H. A. Santos, H. Zhang and X. Zhang, *ACS Nano*, 2025, **19**, 10078–10092, DOI: [10.1021/acsnano.4c16894](https://doi.org/10.1021/acsnano.4c16894).
- 173 L. Zhu, H.-T. Sun, S. Wang, S.-L. Huang, Y. Zheng, C.-Q. Wang, B.-Y. Hu, W. Qin, T.-T. Zou, Y. Fu, X.-T. Shen, W.-W. Zhu, Y. Geng, L. Lu, H.-L. Jia, L.-X. Qin and Q.-Z. Dong, *J. Hematol. Oncol.*, 2020, **13**, 152, DOI: [10.1186/s13045-020-00987-y](https://doi.org/10.1186/s13045-020-00987-y).
- 174 C. Wang, Z. Li, Y. Liu and L. Yuan, *Theranostics*, 2021, **11**, 3996–4010, DOI: [10.7150/thno.56035](https://doi.org/10.7150/thno.56035).
- 175 H. X. Chen, F. K. Bian, J. H. Guo and Y. J. Zhao, *Small Methods*, 2022, **6**, e2200236, DOI: [10.1002/smtd.202200236](https://doi.org/10.1002/smtd.202200236).
- 176 R. Chinnappan, Q. Ramadan and M. Zourob, *Biosens. Bioelectron.*, 2023, **220**, 114856, DOI: [10.1016/j.bios.2022.114856](https://doi.org/10.1016/j.bios.2022.114856).
- 177 H.-L. Cheng, C.-Y. Fu, W.-C. Kuo, Y.-W. Chen, Y.-S. Chen, Y.-M. Lee, K.-H. Li, C. Chen, H.-P. Ma, P.-C. Huang, Y.-L. Wang and G.-B. Lee, *Lab Chip*, 2018, **18**, 2917–2925, DOI: [10.1039/c8lc00386f](https://doi.org/10.1039/c8lc00386f).
- 178 E. Buchan, J. J. S. Rickard, M. R. Thomas and P. G. Oppenheimer, *Adv. Healthcare Mater.*, 2025, e2500122, DOI: [10.1002/adhm.202500122](https://doi.org/10.1002/adhm.202500122).
- 179 S. Liu, F. Zhou, K. Li, S. Chen, B. Hu, Y. Feng, H. Song, X. Lu, D. Wang and C. Ge, *Biosens. Bioelectron.*, 2025, **282**, 117498, DOI: [10.1016/j.bios.2025.117498](https://doi.org/10.1016/j.bios.2025.117498).
- 180 J. Liu, H. Xu, R. Li, J. Lu, Q. Chen, C. Li, L. Guo, W. Chen, L. Zheng, Y. Zhang, T. Wu, H. Chen, W. Han and H. Chen, *Talanta*, 2025, **288**, 127713, DOI: [10.1016/j.talanta.2025.127713](https://doi.org/10.1016/j.talanta.2025.127713).
- 181 C. Martinez-Cisneros, Z. da Rocha, A. Seabra, F. Valdés and J. Alonso-Chamarro, *Lab Chip*, 2018, **18**, 1884–1890, DOI: [10.1039/c8lc00309b](https://doi.org/10.1039/c8lc00309b).
- 182 Y. He, Z. F. Lu, K. Liu, L. Wang, Q. D. Xu, H. L. Fan, C. Liu and T. Zhang, *Sens. Actuators, B*, 2024, **399**, 134851, DOI: [10.1016/j.snb.2023.134851](https://doi.org/10.1016/j.snb.2023.134851).
- 183 J. J. Liu, H. H. Xu, R. Li, J. Y. Lu, Q. Y. Chen, C. H. Li, L. Guo, W. T. Chen, L. X. Zheng, Y. R. Zhang, T. T. Wu, H. Chen, W. H. Han and H. Chen, *Talanta*, 2025, **288**, 127713, DOI: [10.1016/j.talanta.2025.127713](https://doi.org/10.1016/j.talanta.2025.127713).
- 184 Y. Liu, Y. Tan, Q. Fu, M. Lin, J. He, S. He, M. Yang, S. Chen and J. Zhou, *Biosens. Bioelectron.*, 2021, **176**, 112920, DOI: [10.1016/j.bios.2020.112920](https://doi.org/10.1016/j.bios.2020.112920).
- 185 A. I. Barbosa and N. M. Reis, *Analyst*, 2017, **142**, 858–882, DOI: [10.1039/c6an02445a](https://doi.org/10.1039/c6an02445a).
- 186 H. Ben-Yoav, P. H. Dykstra, W. E. Bentley and R. Ghodssi, *Biosens. Bioelectron.*, 2015, **64**, 579–585, DOI: [10.1016/j.bios.2014.09.069](https://doi.org/10.1016/j.bios.2014.09.069).
- 187 Y. T. Zhang, H. C. Gu and H. Xu, *Sens. Diagn.*, 2024, **3**, 9–27, DOI: [10.1039/d3sd00144j](https://doi.org/10.1039/d3sd00144j).
- 188 J. Zhou, J. Dong, H. Hou, L. Huang and J. Li, *Lab Chip*, 2024, **24**, 1307–1326, DOI: [10.1039/D3LC01012K](https://doi.org/10.1039/D3LC01012K).
- 189 M. T. Doganay, P. Chakraborty, S. M. Bommakanti, S. Jammalamadaka, D. Battalapalli, A. Madabhushi and M. S. Draz, *Lab Chip*, 2024, **24**, 4998–5008, DOI: [10.1039/D4LC00671B](https://doi.org/10.1039/D4LC00671B).
- 190 G. M. Hagen, J. Bendesky, R. Machado, T.-A. Nguyen, T. Kumar and J. Ventura, *GigaScience*, 2021, **10**(5), giab032, DOI: [10.1093/gigascience/giab032](https://doi.org/10.1093/gigascience/giab032).
- 191 F. Esmaili, E. Cassie, H. P. T. Nguyen, N. O. V. Plank, C. P. Unsworth and A. Wang, *Bioengineering*, 2023, **10**, 1348, DOI: [10.3390/bioengineering10121348](https://doi.org/10.3390/bioengineering10121348).
- 192 M. Khalghollah, A. Zare, E. Shakeri, B. Far and A. Sanati-Nezhad, *Sci. Rep.*, 2025, **15**, 26415, DOI: [10.1038/s41598-025-11508-7](https://doi.org/10.1038/s41598-025-11508-7).
- 193 J. Park, Y. W. Kim and H.-J. Jeon, *Biosensors*, 2024, **14**, 613, DOI: [10.3390/bios14120613](https://doi.org/10.3390/bios14120613).